Dynamic Mechanical Properties of Complex Blends of Recycled Polymers

William Todd Fielder
Senior Thesis
Physics-Engineering
May 1993

Table of Contents

1.0 Introduction

Presently there is a growing public concern for the health of our environment. One aspect of this concern is the disposal of solid waste. The cost of garbage disposal is ever increasing, and there are environmental problems with the traditional methods of waste disposal. To alleviate some of these problems, recycling has become more and more common. One aspect of recycling that is currently receiving a great deal of attention is plastics recycling; there are many types of plastics, with very different uses and properties, which causes a number of problems when recycling is attempted.[1]

1.1 Role of Plastics in Waste Stream

Plastics are an ever increasing part of our waste stream, principally due to their relatively low cost and advantageous physical properties.[2] Currently, plastics waste comprise approximately 8% of the 150 million tons of municipal solid waste produced annually in the U.S. However, by volume, plastics make up 18% of the municipal waste stream.[3] The major methods of disposing of municipal solid waste, at this time, are landfilling and incineration. However, both of these methods are undesirable for the disposal of plastics. Incineration leads to air pollution, and landfilling of nonbiodegradeable materials, such as plastics, leads to "subsurface land pollution".[4] These problems, and the ever increasing cost of both disposal methods, have lead to recycling efforts. However, plastics, because of their wide range of physical and chemical properties, have been

problematic to recycle.

1.2 Problems with Plastics Recycling

Polymers are hard to recycle because there are numerous polymers that, in general, are immiscible. Most current recycling efforts have focused on a few very common and easily recycled polymers, such as high density polyethylene milk and water bottles and clear polyethylene terephalate soda bottles. These polymers may be easily separated from the waste stream and have a high economic value for recycling.[5]

Most current recycling relies on source or post-collection sorting of the waste, which causes it to be economically unfeasible to recycle all but the most commercially valuable polymers.[6] This problem leads to the landfilling of many consumer plastics. Previous studies have found that it is possible to make low-value items, such as plastic lumber, with feedstocks that do not include the high-value polymers. This study will focus on creating high-value items out of a feedstock of polymers with very little separation and sorting.[7] Now it is necessary to give a detailed explanation of why most polymers form immiscible blends.

1.3 Thermodynamics of Miscibility

Most combinations of high molecular weight polymers are immiscible.

> That is, when mixed together, the blend components are
> likely to separate into phases of predominately their
> own kind. This characteristic, combined with the often
> low physical attraction forces across the phase
> boundaries, usually causes immiscible blend systems to
> have poor physical properties.[8]

Inspite of this fact, useful combinations of immiscible polymers may be made using compatibilizers. The term miscibility has the same meaning in the description of polymer blends as it does for blends of lower molecular weight components. For example - "alcohol and water are miscible but oil and water are not."[9] The main problem when forming systems of multicomponent polymer blends, is to achieve good stress transfer between the components.

The reason various types of plastics are immiscible lies in thermodynamics. The degree of miscibility of any mixture is controlled by the Gibb's free energy of mixing, ΔG_{mix} which is defined as

$$\Delta G_{mix} = \Delta H_{mix} - T\Delta S_{mix}$$

where ΔH_{mix} is the change in enthalpy from mixing and ΔS_{mix} is the entropy change due to mixing. There are three possible curves for the free energy of mixing versus the volume fraction ϕ of the component.[10] Figure 1 shows these three possibilities of ΔG_{mix} versus component ϕ_2 of a two component mixture. Curve 1 shows the case of a completely immiscible blend, because the free energy of mixing is always positive; the components of this mixture are not miscible to any extent. Curve 2 shows a mixture of completely miscible components, because the free energy of mixing is negative in all cases. However, this condition is not the only one for a completely miscible blend. Curve 3 shows a

mixture where the free energy is always negative, but it is increasing in the center. This blend is a partially miscible blend. There are two conditions for complete miscibility that may be stated as follows:

$$\Delta G_{mix} < 0$$

$$\left(\frac{\partial^2 \Delta G_{mix}}{\partial \phi_2^2} \right)_{T,P} > 0$$

Both of these conditions must hold for the mixture to be completely miscible. These two conditions are the only "thermodynamically valid definition of miscibility", but there are many models that allow easier calculations based on estimates of some terms, because the Gibb's Free Energy can not be directly measured.[11] [12] A description of these simplifications may be obtained from either of the references for this section, but is not included here, because a detailed study of computational thermodynamics is not the purpose of this section.

Paul and Barlow's Polymer Blends (or Alloys) provides a very good example of why polymers are much harder to mix than other smaller molecules. Imagine a square filled with 50 blacks dots and 50 white dots that are randomly distributed. It is very easy to compute that there are 10^{30} possible combinations. If you connect each type of dots into five chains with ten dots each, the number of possibilities is reduced to 10^3. This example shows the problems of mixing the long polymer chains of two

different types of polymers.[13]

This brief discussion demonstrates some of the problems with mixing of polymers and the thermodynamic reasons behind them. There are very few combinations of polymers that exhibit the characteristics of complete or partial miscibility. When a complex multicomponent feedstock is used, immiscibility is assured. These problems are the reasons the study of polymers made from unseparated, recycled feedstocks is so interesting and challenging. The focus of this study is to determine how to make better high value polymers samples out of such unseparated, recycled feedstocks. This paper studies some very specific attempts at using compatibilizers to enhance the properties of samples made from recycled feedstocks, rates their effectiveness, and determines the causes of their mechanical properties.

2.0 Feedstock

All polymer samples in this study were fabricated from post-consumer plastic waste. The feedstock that is the focus of this paper is called the Model Cities (MCC) feedstock, and is described in detail below.

2.1 Major Components of Feedstock

The material for the MCC feedstock was collected in 1990-1991 by the Center for Plastics Recycling Research (CPRR) in Highland Park, NJ. Participants in 102 homes were asked to separate all clean plastic items from their garbage, to represent the mixture of plastics obtained without any source separation or post-collection sorting. The mixture of plastics obtained was

approximately, by weight: plastic bottles, 60%; rigid containers, 10%; and plastic film, 10%. The plastic film portion of the collected plastics was approximately: 95% polyethylene (shopping bags, garbage bags, cereal and cookie bags, etc.), 1% polypropylene (clothing bags), and less than 1% polyvinyl chloride, laminated food wrap, cellophane, and others.[14] The polymer components of this mixture, prior to any modifications, are: polyethylene terephalate (PET) soft drink bottles, 20.3%; other PET containers, 3.5%; high-density polyethylene (HDPE) milk and water bottles, 17.6%; pigmented HDPE, 20.0%; thermoformed polystyrene (PS) containers, 2.5%; PS foam (trays, cups egg cartons, packing material), 2.3%; film, 13.3 %; polyvinyl chloride bottles, 1.9%; polypropylene (PP) bottles, 0.7%; composite bottles, 0.5%; tubs (PS, HDPE, PP), 4.4%; and miscellaneous (toys, flower pots, car mats, appliances, laundry baskets, buckets, hangers, etc.), 13.5%.[15] [16]

The MCC mixture was not processed exactly as it was collected: the miscellaneous component of the mixture was found to contain large metal objects, and was therefore dropped from the study. The polymeric components of the MCC feedstock after this modification are as follows: PET, 28%; natural (translucent) HDPE, 21%; colored HDPE, 23%; PS, 9%; film, 15.5%; PVC, 2%; PP, 1%; and composite bottles, 0.5%.[17] [18]

2.2 General Properties of Major Components

To gain an understanding of the very different nature of the major components of the MCC feedstock, I will give the chemical

structure and some properties for the major components of the feedstock. I will give a detailed explanation of the properties of PET and HDPE, and a briefer description for PS.

2.2.1 PET

PET is a polyester made from the reaction of terephalic acid and ethylene glycol.[19] The chemical formula for a PET mer is shown in figure 2. Here are some of the important properties of PET: It has a specific gravity of 1.37. It melts or decomposes at a temperature of 265 °C (slightly higher for a very crystalline sample). It has a very good abrasion resistance, and is resistant to acids, bases, solvents, and oils and fats. It has an elongation between 50 and 300%, a notched impact strength of 4 J/mm, and did not break in the unnotched impact test.[20] However, it is necessary to be very careful to dry and crystallize PET at the same time to prevent hydrolysis reducing the molecular weight. PET is a very hydrophilic polymer at higher temperatures, such as those used for molding.[21]

2.2.2 HDPE

PE is the polymer produced by addition polymerization of ethylene. The chemical formula for a PE mer is given in figure 2. PE has both amorphous and crystalline portions, and the degree of crystallinity influences the properties and use of PE. The crystallinity is controlled by the number of side branches. HDPE is characterized by fewer side branches, and is more crystalline.[22] HDPE has a specific gravity of 0.94 to 0.96. It has a melting or decomposition temperature of 135 °C. It has

very good impact properties; neither the notched or unnotched samples broke. Its elongation is between 15 and 100%. It has poor abrasion resistance, and good resistance to acid, bases, solvents, oils and fats, and bacterial and fungal attack, but poor resistance to sunlight.[23]

2.2.3 PS

PS is a hard, glassy amorphous polymer, made from a chain of carbon atoms, with phenol side groups.[24] The chemical formula of a mer is given in figure 2. It has a specific gravity of 1.05, low impact strength for both notched and unnotched tests, and low elongation.[25]

2.3 Preparation of MCC Feedstock

The MCC feedstock, after the removal of the miscellaneous component, was processed in the CPRR-Rutgers resin recovery plant, where metal chips from bottle caps are removed and the plastics are chipped and washed. Then, the mixture is dried to minimize degradation, especially of the PET component. Next, this mixture is fed into a 51 mm counter rotating non-intermeshing twin-screw extruder (CRINI TSE) manufactured by Welding Engineers. This extruder melts, compounds, filters, degases, and pelletizes the polymers. The goal of this compounding is two-fold: (1) to create a microdispersion of the minor components in the polyolefin matrix, and (2) to draw the stiffer main components into fibers. The processing temperatures of the MCC feedstock do not exceed 250 °C. The CRINI TSE extruder is able to feed very low bulk density materials,

minimizes metal-to-metal contact areas, and has wide feed and vent openings. The melt filter used was an in-line screen cleaner whereby a small portion of the flow through one screen could backwash the other within seconds. The filter incorporated a valve mechanism to allow uninterrupted product flow as one screen pack was backwashed or inspected.[26] [27]

The pellets produced in the CRINI TSE were further modified at the Polymer Processing Institute (PPI) by compounding in a 30 mm co-rotating TSE (the ZSK 30 by Werner and Pfleider) with commercial elastomers. The concentrations of these elastomers varied from 1 to 10% by weight. The compounded pellets were injection molded in a Van Dorn 40 machine equipped with an ASTM specimen mold. Molding parameters were varied in an attempt to produce samples with good surface appearance.[28] The two primary conditions may be summarized as follows: (1) condition A, characterized by lower melt temperature (165-180 °C), higher mold temperature (85 °C), fast injection speed, short cycle, and slow screw speed; and (2) condition B, characterized by higher melt temperature (205-218 °C), lower mold temperature (50 °C), slow injection speed, longer cycle time, and slower screw speed. Condition B produced samples with poor surface appearance, while condition A produced samples with good surface appearance.[29] [30]

2.4 Naming of MCC Feedstock Samples

Before a further explanation of the research can be undertaken, it is necessary to explain the naming conventions for this paper. First, all Model Cities sample start with MC, and

samples that have been compounded have a second C (MCC). All of the samples referred to in this paper are compounded. Second, the last letter refers to the molding condition (A or B). Third, any intermediate letters refer to the compatibilizer added to the mixture, EP, EPX, SI, or SEBSX. Fourth, the number before the label of the compatibilizer refers to its weight percent in the mixture. For example, MCC-A is unmodified, compounded Model Cities molded at condition A, MCC-5SI-B is Model Cities modified with 5%, by weight, of compatibilizer SI molded at condition B. Likewise, MCC-10EP-A is Model Cities with 10% of compatibilizer EP molded at condition A.

The compatibilizers used in this study are four different commercial compatibilizers. The name used in this study, general chemical composition, commercial name, and manufacturer are listed below: (1) EP, ethylene-propylene copolymer, VISTALON ® grade with a minimum 60% ethylene content, Exxon Chemical; (2) EPX, modified ethylene-propylene copolymer, EXXELOR ® VA 1803, Exxon Chemical; (3) SI, styrene block copolymer, pilot plant version of the recently commercialized VECTOR ® 6100-D, Dexco Polymers; and (4) SEBSX, modified styrene-ethylene/butylene-styrene block copolymer, KRATON ® FG1901X thermoplastic rubber, Shell Oil Company.[31] [32]

2.5 Properties of MCC Feedstock

Here is a summary of the characteristics of the refined commingled pellets produced by the CRINI TSE. The mixture was tested for chemical composition using several different methods.

First, the pellets were subjected to solvent extraction. Approximately 8.4% of the mixture, the styrenic portion, was soluble to benzene, 56.6% to boiling xylene, the polyolefin portion, and 35%, composed of PET and other polymers, was insoluble. Second, infrared spectroscopy revealed that the pellets are a complex mixture composed of PE, PP, PET, PS, and polyvinyl chloride. Third, differential scanning calorimetry (DSC) was used to reveal several heating peaks associated with the melting points and glass transitions of the various components of the mixture. DSC also revealed two cooling peaks. This data is not included in this paper, because it is unimportant for the analysis in the paper. The complete data may be obtained from the references for this paper.[33]

The acid number, the portion of the pellets soluble in hot xylene, is 2.34 mg KOH/g of sample. The melt flow rate as received was between 3.9 and 4.4 g/10 min., and was 6.8 g/10 min. after one pass through the TSE. The apparent viscosity of the pellets was also studied at two different temperatures. The pellets were also analyzed using an isothermal thermogravometric analysis. The data from these two experiments may also be found in the references to this paper.[34]

The complex chemical composition of the multicomponent mixture reflects the variety of items and resins in the original recycling stream. Samples of injection molded plastics are fairly brittle with low elongation and impact strength; their modulus and strength values did not approach those of virgin

(pure, non-recycled) HDPE. A second pass through the ZSK 30 did not result in appreciable changes in mechanical properties (data not shown). Similarly, the choice of injection molding conditions affected only the surface appearance and to a certain degree morphology, but had little effect on the mechanical properties of the unmodified plastics. Low temperature and short cycle (condition A) produced good surface appearance. Higher temperature and longer cycle (condition B) produced white patches on the surface, presumably as a result of degradation of some components of the mixture. Infrared Spectroscopy confirmed the presence of polyvinyl chloride and/or polyvinyl dichloride related structures (possibly degraded) along with species containing nitrile groups; polymers containing the later are known for affinity and compatibility with chlorinated polymers.[35]

The properties produced by adding 5 and 10%, by weight, of the modifiers were studied. The effects that are usually associated with impact modification, i.e. reduced modulus, strength and deflection temperature under load, and increased impact strength and modification are quite pronounced for the styrenic block copolymer (SI) and to a lesser extent for the modified styrene/olefin block copolymer (SEBSX). Both modified and unmodified ethylene-propylene copolymers (EPX and EP respectively) do not appear to offer significant improvements. Therefore, their study was not continued.[36]

Here are some examples of the experimental data that allows this conclusion: The stress at yield in MPa: MCC-B, 22.6; MCC-

A, 22.7; MCC-5EP-B, 19.7; MCC-5EPX-B, 19.4; MCC-5SI-B, 17.8; MCC-10SI-A, 15.7; MCC-5SEBSX-B, 21.4; MCC-10SEBSX-A, 19.2. The stress at break in MPa is: MCC-B, 22.3; MCC-A, 22.5; MCC-5EP-B, 19.3; MCC-5EPX-B, 19.0; MCC-5SI-B, 16.4; MCC-5SI-A, 17.9; MCC-10SI-A, 12.7; MCC-5SEBSX-B, 19.6; MCC-5SEBSX-A, 21.7; and MCC-10SEBSX-A, 18.8. the elongation at break in % is: MCC-B, 3.0; MCC-A, 3.33; MCC-5EP-B, 4.9; MCC-5EPX-B, 4.4; MCC-5SI-B, 10.4; MCC-5SI-A, 5.2; MCC-10SI-A, 24.1; MCC-5SEBSX-B, 9.3; MCC-5SEBSX-A, 4.6; and MCC-10SEBSX-A, 5.1. The initial modulus of each sample in MPa is: MCC-B, 1100; MCC-A, 1100; MCC-5EP-B, 908; MCC-5EPX-B, 919; MCC-5SI-B, 763; MCC-5SI-A, 1030; MCC-10SI-A, 785; MCC-5SEBSX-B, 818; MCC-5SEBSX-A, 1240; and MCC-10SEBSX-A, 1010.[37]

At this point, it is very easy to see how the compatibilizers EP and EPX have very little effect on the properties of the polymers, therefore their study will not be continued in this paper. It is also easy to see how the data does differ for the modified samples molded at the different conditions. Condition A will be the focus of this paper and all of the mechanical data presented in the rest of this section will be for molding condition A samples unless stated otherwise. The condition B samples will not be studied in as much detail, because of their poor surface appearance. Also, in contrast with the unmodified refined commingled plastics, the choice of molding conditions seems to affect the properties of these compounds. Modified materials molded under condition B appear to have higher elongation and unnotched impact, but lower modulus and strength.

However, the data for condition B samples follows the same trends as the data for condition A samples, but the actual values for the properties is different.[38]

The notched impact strength of the samples in J/m is: MCC, 58.7; MCC-5SI, 48.0; MCC-10SI, 139; MCC-5SEBSX, 37.4; MCC-10SEBSX, 58.0. The unnotched impact strength of the samples in J/m is: MCC, 128; MCC-5SI, 374; MCC-10SI, sample did not break; MCC-5SEBSX, 224; MCC-10SEBSX, 272. The deflection temperature under a load of 1.82 MPa in °C is: MCC, 59.5; MCC-5SI, 53; MCC-10SI, 47; MCC-5SEBSX, 55.5; MCC-10SEBSX, 49.[39]

The addition of elastomeric modifiers significantly affects unnotched impact and Gardner impact strength, but only marginally notched impact strength. The presence of skin/core structures (See figure 3) having different morphology and/or composition could be responsible for this behavior. Also, the presence of different microstructures formed during molding may result in the observed dependence of properties on the choice of molding conditions. Microscopic examinations of fracture surfaces confirm that the presence of all elastomeric modifiers produces skin/core morphologies, which seem to be more pronounced under condition B. Modified samples, in general, showed finer morphologies that the unmodified ones. In addition, increasing the concentrations of SI and SEBSX resulted in increased ductility.[40]

3.0 Dynamic Mechanical Analysis (DMA)

DMA involves the testing of a material under a wide range of

temperatures or frequencies to study is behavior.

3.1 Types of DMA

Dynamic mechanical analysis may be performed with various types of machines, which operate on different principles. There are four major types of dynamic mechanical methods that are routinely used with polymers: the torsion pendulum, the resonant rod, the ultrasonic method, and the forced-oscillation method.[41]

In the first method, the torsion pendulum, a specimen is clamped rigidly at both ends, twisted via an inertial arm, and released. The decay of the oscillations is then recorded. Dynamic mechanical data may be obtained from the decay of the oscillations using equations not listed here.[42]

The second method is the resonant rod. Three types of vibration, longitudinal, torsional, and flexural, are possible with this method, depending upon the setup of the machine used.
[43]

> In longitudinal vibration the elements of the rod
> expand and contract parallel to the axis, which is
> parallel to the direction of wave propagation. In
> torsional vibration the elements oscillate around the
> axis of the rod. In flexural vibration the elements
> are translated at right angles to the axis of the
> rod.[44]

Dynamic mechanical information may be calculated from the resonance peaks obtained through this analysis.[45]

Third, there is the ultrasonic method, where a pulse of sound is transmitted through the sample. There are several ways in which the sound may be transmitted, each has its own equations which will not be discussed here.[46]

The final method of DMA involves the use of forced-oscillations.[47] In the forced-oscillation method, a sinusoidal strain is applied to a material and its response is studied over a wide range of temperatures or frequencies. For a completely viscous material the stress is 90° out-of-phase with the applied strain; for a completely elastic material the stress is completely in-phase with the strain. Polymers and polymer blends are viscoelastic materials, reacting somewhere between the two extreme cases of completely viscous and completely elastic materials. Polymers have a phase angle δ between their stress and strain vectors, τ^* and γ^* respectively.[48]

To analyze the results of a dynamic mechanical test, there three very important variables to study. The first is the storage or in-phase modulus, which is defined as

$$G' = \frac{\tau'}{\gamma'}$$

where the prime (') refers to the in-phase component of the stress and the strain vectors. The out-of-phase or loss modulus is defined as

$$G'' = \frac{\tau''}{\gamma''}$$

where the double prime (") denotes the out-of-phase component of the vectors. The third variable to study is tan δ, the tangent

of the phase angle. It is defined as

$$\tan\delta = \frac{\tau''}{\tau'} = \frac{G''}{G'}$$

[49] There are other variables that may be calculated using the results of DMA, but the most common ones are the loss modulus, the storage modulus and tan δ, so I will confine my discussion to them.

3.2 Method of DMA Used in this Study

The forced-oscillation method is the one used at Washington and Lee University (W & L). There are many types of forced-oscillation machines which apply the sinusoidal load in many different ways, some work over a wide frequency range, others over a wide temperature range. I will not attempt to explain the workings of these machines. The machine is used at W & L is the computer controlled Perkin Elmer Dynamic Mechanical Analyzer 7 (DMA7). (See figure 4) The DMA7 may apply the forced-oscillations to the sample by the means of various measuring systems. The measuring system may be changed by making a few minor equipment changes. The measuring systems available for use with the DMA7 are: three point bending, film extension, fiber extension, parallel plates, single cantilever, and double cantilever. In three point bending, the sample is placed on two "knife edges", thin supports that round the depth of the sample, and is loaded in the center. In film and fiber extension, the film or fiber is clamped at the top and bottom and then

stretched. Parallel plates are used for very soft material; the sample is placed between two circular flat plates and then compressed. In the two cantilever arrangements, single and double, the sample is supported by a cantilever support, at one or both end, respectively. There are several types of sample mounting arrangements available with certain measuring systems to accommodate various sample sizes. The type of measuring system used depends upon the material properties of the sample and the temperature range the sample will be subjected to.[50]

The measuring system used for the data presented in this paper is three-point bending. The sample is placed on two knife edges and is loaded in the midway between the edges. (See figure 5) For a further explanation of the measuring system, sample size and placement see the sample preparation section of this paper. (Section 4)

3.3 Possible Uses of DMA Data

DMA is very useful because of the information that may be obtained from studying the loss modulus, the storage modulus, and tan δ.

> The investigation of the dynamic [storage] modulus and the internal friction [tan δ] over a wide range of temperatures and frequencies has proved very useful in studying the structure of high polymers and the variations of properties in relation to end use performance. These dynamic parameters have been used to determine glass transition region, relaxation spectra, degree of crystillinity, molecular orientation, crosslinking, phase separation, structural or morphological changes resulting from processing, and chemical composition in polyblends, graft polymers, and copolymers.[51]

3.4 Glass Transition and Melting Point

DMA can be used to study polymers over a wide temperature range, which is very important, because the properties of polymers are temperature dependent. For example, plastics may be hard at room temperature, but become more flexible as they are heated.

There are two very important temperatures common to all polymers: the glass transition temperature, T_g, and the melting point, T_m. The melting point is self explanatory and is not unique to polymers. However, one feature of polymers that distinguishes them from other materials is the glass transition temperature. Below T_g polymers are hard, brittle, and generally glass-like, while above this temperature they become softer and more flexible. When a polymer is below T_g, there is insufficient energy for the polymer molecule to overcome the barriers for rotational and translational motion. Segments of the polymer molecule are locked into place. However, above T_g there is sufficient energy for the polymer to undergo micro-Brownian motion and for chain segments move freely. The T_g of the polymer may be determined from an abrupt change in the data from DMA. The T_g of a polymer appears as a rapid decrease in the storage modulus, and peaks in the loss modulus and tan δ.[52]

Each polymer has its own T_g and T_m. Here is a list of T_g and T_m, respectively, for some important polymers (in °C): PE, -120, 136; PS, 100, 240; PET, 69, 265. In most cases T_m and T_g are related, because they are affected similarly by features in the polymer structure. For asymmetrical polymers T_g equals

approximately two-thirds T_m, and for symmetrical ones T_g equals approximately half T_m, if both are in Kelvin.[53]

All polymers experience additional relaxations (also called transitions or dispersions) that may be observed on the DMA curves for the polymer. There may be α-, β-, γ-, and δ-relaxations in some polymers.[54]

3.5 Relaxations of Major MCC Components

In the following section I will present DMA information on the major components of the MCC feedstock. For more information on the feedstock used in this study see the feedstock section of this paper. (Section 2) I will present the fundamental DMA information for HDPE, PET, PS, and PP; this information is critical for understanding the results from the more complicated multi-component polymers produced from the MCC feedstock and various compatibilizers.

3.5.1   HDPE

HDPE is the most prevalent polymer in the MCC feedstock. It makes up 44% of the entire feedstock, as processed. HDPE has four major relaxations, the α, α', β, and γ. All of these relaxations may be seen on the plot of the storage and loss moduli and tan δ (figure 6) for HDPE.

The α-relaxation occurs at temperatures very close to the melting point of HDPE (approximately 110 °C) when DMA is preformed at 1 Hz, and may not be observed at frequencies above 100 Hz. The most plausible explanation for this relaxation is a boundary phenomenon similar to grain boundary slip in metal, but

this hypothesis has not been proven yet.[55]

The second relaxation for HDPE is the α'-relaxation which is just a knee in the curve (compared with a distinct relaxation for low density PE). This relaxation occurs at approximately 75 °C. The α'-relaxation is caused by "vibrational and reorganizational motion within the crystals of the polymer." It does not occur unless crystals are present in the sample and is a function of the chlorine content of the polymer sample.[56] Its temperature is lowered by changing the comonomer content and side branch content in a way that lowers T_m, and by quenching. Annealing raises the temperature of the α-relaxation.[57]

The β-relaxation occurs at approximately -15 °C. The magnitude of this relaxation depends on the number and type of side branches in the HDPE; the different types of side branches have different effects.[58] This relaxation is due to the relaxation of the branch points, particularly the portions containing a side group. The γ-relaxation occurs at approximately -115 °C, and is the amorphous regions glass transition. It is primarily a function of density; as the density of HDPE increases the magnitude of the peak decreases.[59]

3.5.2   PET

PET is the second largest component of MCC, making up 28% of the feedstock prior to processing. PET has a T_m of 260 °C and a T_g of 67 °C for amorphous samples and approximately 80 °C for crystalline samples.[60] PET has two relaxations an α-relaxation and a β-relaxation. Figure 7 shows the storage and loss moduli

and tan δ for PET.

The α-relaxation is dependent on the degree of crystallinity of the sample. The peak occurs at approximately 80 °C for a low crystallinity sample, while it occurs at approximately 105 °C for a very crystalline sample. "The magnitude, location and breadth of the α-relaxation in PET are a function of the degree of crystallinity and also the manner in which the a particular degree of crystallinity is obtained."[61] A much more detailed description of the dependence of the α-relaxation on crystallinity may be obtained by reading several of the references for this paper, but a detailed description is not needed for the analysis in this paper.

The β-relaxation of PET occurs at approximately -55 °C. The location of β-relaxation is independent of the crystallinity of the sample, however its magnitude decreases slowly with increased crystallinity. The relaxation is thought to be associated with both the crystalline and non-crystalline regions of the polymer. Many different hypotheses have been developed to explain the β-relaxation, but none has been proven to be the correct one.[62]

3.5.3   PS and PP

I will devote much less time to the explanation of the mechanical behavior of PS and PP because they appear in much smaller percentages in the MCC feedstock. Both amorphous and crystalline PS have an α-relaxation at 116 °C. In crystalline PS there is also a β-relaxation at 50 °C, a γ-relaxation at -125 °C and a δ-relaxation at -235 °C.[63] PP has an α-relaxation at 75

°C, a β-relaxation at 10 °C and a γ-relaxation at -80 °C.[64]

3.6 Transitions of a MCC Polymer Related to its Major Components

Before undertaking any complicated analysis of samples from the MCC feedstock, it is necessary to understand how the transitions of MCC polymers relate to the transitions of its major components. Figure 8 is a plot of the loss modulus, storage modulus, and tan δ for virgin (pure, non-recycled) HDPE, virgin PET, and an uncompatibitilized MCC polymer. At this time it is unimportant whether MCC-A or MCC-B is used, because the purpose of this section is to show, in a general manner, how the transitions of MCC come from its major components. The same principle holds when compatibilizers, and their relaxations, are added to MCC polymers. It is very important to realize when looking at the curves in figure 8 that we can only compare the shapes of the curves for the three different polymer samples, not the magnitudes. The reason for this limitation is that we are studying the curves for virgin HDPE and PET that are not necessarily of the same composition as the components of MCC. The temperatures of the various transitions do not correspond exactly between the virgin and recycled material, but this fact does not cause a problem, because the purpose of this section is for the reader to get a feel of how the transitions of MCC and its components are related. The later sections of this paper deal with a much more detailed analysis of the three main curves for various formulations of MCC polymers.

The first transition to study is the HDPE γ-relaxation at

approximately -120 °C. This relaxation is easiest to see on the loss moduli of both polymers; the peak of the HDPE curve is at almost the same temperature as the peak on the MCC curve. It is also easy to see the same effect with the changing slopes of the storage moduli for both of these samples. The slopes for HDPE and MCC both change from a steep negative slope to a relatively flat one at approximately the same point. The same principle holds true with tan δ, but the peaks are farther apart and the effect is much harder to see, because of the relatively low values of all three tan δ's.

The next relaxation to study is the PET β-relaxation at -80 °C. This value is lower than the one given earlier in this paper and many books, most likely because we used a different method of DMA (three point bending). It is possible to see that this relaxation must be the β-relaxation for PET, since there are no relaxations for other major MCC component in this region. The effect of PET relaxation on the MCC curve is less pronounced, because PET is the second largest component of MCC, at 28%, compared with 44% for HDPE. Again, the first curve that will be studied is the loss modulus, and it is easy to see how the PET peak starts to affect the loss modulus of MCC at approximately -110 °C. Below this temperature, the slope of the loss modulus of MCC is steep and negative, just as with HDPE, but as PET approaches and reaches its relaxation, the slope becomes much flatter. It is very easy to see how the relaxation of PET helps to negate the properties of HDPE in this region. This same

effect is also evident when comparing the storage moduli of the three polymers. The tan δ of MCC does not drop like HDPE's, because the tan δ of PET is increasing and negates the fall of tan δ of PET.

HDPE has its second relaxation at approximately -15 °C, and this relaxation takes the form of a valley in the loss modulus and tan δ and is barely evident in the storage modulus. This HDPE relaxation shows up as a valley in the MCC curve at approximately -10 °C and is very difficult to find in tan δ and the storage modulus. HDPE has another relaxation at approximately 50 °C for the sample studied here. This relaxation is evident in all three of the curves for this polymer. It is a peak in loss modulus, a flattening of the negative slope of the storage modulus, and an increasing positive slope for tan δ. The effects again appear in the curves for MCC. There is a broad peak in the loss modulus of MCC from approximately 25 to 80 °C. The beginning portion of this peak may be attributed to the HDPE relaxation. There is a small change in the slope of MCC's storage modulus at this point, but it is hard to see. The effect of the HDPE relaxation is much more evident as an increase in the positive slope of tan δ for MCC.

At this point, the reader should be able to recognize the PET transition at 75 °C, so I will not describe its appearance here. However, I will mention that it appears in MCC as the latter portion of the broad peak in the loss modulus and as the final increase of slope in the tan δ of MCC. The storage modulus

of MCC does not show a fast drop like the storage modulus of PET, because the effects of HDPE negate it. The most important feature to notice in this region is how the MCC loss modulus has one very broad peak in this region, resulting from the effects of a HDPE relaxation and a PET relaxation. The storage modulus, and tan δ show the same type of combining of the relaxations of the two major components, but it is not as obvious.

It is very important that the reader sees and understands how the nature of the two major components of MCC is reflected in the three DMA7 curves for MCC polymers. If this fact is not clear at this point, the reader should re-read this section until a understanding of this relationship is reached. The fact that such a relationship exists is the basis of much of the latter portions of this paper. This section will be useful later in the paper when trying to distinguish the effects of the compatibilizers from those of the components of MCC. The reader should now be comfortable at looking at multiple DMA7 curves and trying to relate them, because this will be done throughout the paper and most conclusions reached will be based on DMA7 data presented in this form.

4.0 Sample Preparation

Careful preparation and mounting of samples for the DMA7 is critical for obtaining accurate and consistent results. Polymers begin to deform when they are heated rapidly, and this deformation changes the mechanical properties of the polymer, and thus the results obtained from the DMA7. Accurate measurements

of the sample dimensions are also important; if the sample
dimensions are incorrect, all of the curves calculated by the
DMA7 will show the correct shape, but with incorrect magnitudes.
Consistency in measurement technique is also important, because
the polymer samples are relatively soft and flexible at room
temperature, and, if the dimensions are not measured carefully,
vastly different readings may be obtained from several trials.
It is very important to tighten the micrometer to the same
resistance (from the polymer) to obtain consistent results.
Other researchers have also realized that sample preparation and
mounting are critical for obtaining accurate and consistent
results, and have pointed out possible sources of error for
various types of forced-oscillation DMA study.[65]

4.1 Sample Orientation

The polymers from which the samples will be made arrive at W
& L in dogbone form, as shown in figure 9. For a description of
the feedstock used and its preparation, see the feedstock section
of this paper. (Section 2) After the type of polymer to be
studied has been selected, it is necessary to decide which
orientation to study, as the properties of polymers vary
depending upon which part of the dogbone is tested. The
orientations that we have studied at W & L are either
perpendicular, or parallel to the long axis of the dogbone.
Parallel samples are either cut from the outside, or skin, of the
dogbone or the inner core. All of these orientations are shown
in figure 9.

The parallel and perpendicular in the orientation names refer to whether the sample is parallel or perpendicular to the direction of the polymer flow into the mold during processing. The parallel outside pieces contain three outer sides. These outer sides are one outside edge of the dogbone, and a section each of the top and bottom of the dogbone. The parallel core pieces contain no outer sides as both the top and bottom are removed before the sample is cut. No variations of the perpendicular orientation have been studied.

4.2 Sample Milling

All of the polymer samples for the DMA7 must be approximately 2 mm X 3 mm X 19 mm; these dimensions conform to the set up of the machine and allow the necessary stress to be applied to the sample without reaching the limit of the machine. The samples for the DMA are initially prepared to rough dimensions using a Hardinge milling machine and a 4" X 1/16" circular slitting saw blade. First, the preparation of parallel outside pieces will be explained in detail, and then the modifications of the process that are necessary to prepare the other orientations will be explained.

4.2.1 Parallel Outside Pieces

The first step in preparing a parallel outside sample is to cut a section of the dogbone from the smaller middle section, away from the curves at each end, using a band saw. The length of this piece should be approximately 45 mm, so two samples may be cut from it. Next, the edge of the dogbone opposite from

where the sample will taken must be made even. After this edge

is prepared, the sample is mounted in a "jig", to hold it

perfectly still and perpendicular to the blade. This jig was

made at W & L in the machine shop specifically for this purpose;

it is shown in figure 10. The piece from the dogbone is then

placed into the jig with a thin lower support and a thicker upper

support that is tightened against the sample using two set

screws. The upper support is made of aluminum, just as the jig

is, and the lower support is a thin strip of brass. Brass was

chosen for the lower support, because it will not damage the saw

blade if the blade accidently contacts it.

After the sample is properly positioned and securely mounted

in the jig, the jig is placed in the vise on the milling machine.

Next, the vice is moved until the blade is just above the brass

shim. Then the vise is moved until the blade just touches the

outside edge of the sample in the jig. The vise is moved back

and forth until blade runs along the entire edge, if this does

not happen, the vise is moved closer to the edge. The purpose of

this process is to assure that the outside edge will be perfectly

parallel to the cut which removes the sample.

Then, the blade is raised until the blade will clear the

sample in the jig. Next, the blade is moved in 143/1000 in. (2

mm plus the blade width). This movement of the vise must be done

carefully so that the blade is not moved in the wrong direction,

because this reversal of direction will change the calibration of

the measuring system on the milling machine and require the

repeating of all the steps from where the blade is initially
brought into contact with the sample. Next, the blade is
lowered so it just barely contacts the sample. The vise is then
moved so that the blade no longer touches the sample, and the
vise is raised 25/1000 in., and the automatic table movement
control is engaged. The blade is allowed to run the entire
length of the sample, and then the table movement is stopped.
The vise is brought back to the starting position for this
portion of the process, so the blade is not touching the sample,
and the blade is lowered 25/1000 in., and the process is
repeated. This process is repeated until a depth of 110/1000 or
115/1000 in. out of 118/1000 in. (or 3 mm) is reached. The jig
is removed from the vise and the remaining strip connecting the
DMA sample to the rest of the piece is removed with a razor
blade.

It is necessary to raise the vise in such small intervals to
avoid heating and deformation of the polymer. If the sample
begins to warp at 25/1000 in., the interval must be decreased or
compressed air must be blown against the blade and the sample to
dissipate the heat. If the sample becomes too deformed, the
results from DMA7 analysis might be inaccurate, or in an extreme
case, it might not even be possible to run the sample in the
DMA7.

4.2.2 Other Orientations

The preparation of the other orientations requires slight
modifications of the process given earlier. For example, to cut

a perpendicular piece you start with the wide end of the dogbone, make one complete cut, and then move over 143/100 in. and make another complete cut. The preparation of parallel core piece is more involved, requiring the shaving of the outside layer on each side and the making of two interior cuts to produce a sample 3 mm wide. The shaving process involves mounting the sample on a platform of aluminum and brass, attaching the piece to be shaved to the brass with hot glue. A much wider saw blade (¼") is used to remove 0.5 mm from each side of the piece. After this shaving of the sample is completed, the two cuts may be made, using the narrow saw blade, to produce a 3 mm wide sample. The hot glue does not damage the sample for the DMA7, because it is far enough away from where the sample is cut.

4.3 Final Preparation for DMA7 Study

Next, the roughly prepared sample must be prepared for the DMA7 and then mounted in it. During the final preparation the sample is carefully reduced in size with a razor blade until it has a maximum variation in height and depth of approximately ±0.1 mm. Each edge of each side is checked to make sure the sample is not higher or wider on one edge compared with the other. Then, the length of the sample is cut to approximately 19 mm so there is extra room when positioning the sample on the knife edges. The final step of the final preparation is to use magnifying goggles to make sure there are no frayed edges that will distort the measurements or cause the sample to not sit securely on the knife edges.

4.4 Sample Mounting in DMA7

The final step is to position the sample at the center of
the knife edges on the DMA7, in order that the measurement
designated as the depth is the side that is approximately 3 mm
and the one called the height is the side that is approximately 2
mm. Once the sample is centered an appropriate stress is applied
to the sample, a check is made using the magnifying goggles to
see if the sample rocks (wiggles back and forth on the knife
edges). If rocking occurs, the additional motion will cause the
DMA7 data to be inaccurate and the sample must be further
prepared and remounted until the rocking is eliminated. In
addition to the check for rocking, the operator of the DMA7 must
check to see if the probe makes continuous contact with the
sample. After all of these factors are checked, the operator may
begin the run.

4.5 DMA7 Operating Conditions

All of the DMA7 runs for this paper were performed under the
same set of operating conditions. First, the runs were over a
temperature range of -155 to 110 °C, which was dictated by the
transitions of the major components of the MCC feedstock. The
temperature was raised at a constant rate of 3 °C/min. This
temperature rate is maintained by the DMA7 through the use of
liquid nitrogen (-190 °C), which is placed in a reservoir
surrounding the sample, knife edges, and probe, and a furnace.
Second, all runs are performed at a frequency of 1 Hz; the
frequency is the rate at which the probe moves up and down to

load and unload the sample in DMA. Third, all runs are preformed at a constant strain rate. This rate was usually 0.040%, but sometimes it was necessary to reduce the rate by 0.001 to 0.002% so that the stresses to be applied were with in the limits of the machine. (When the strain is set to a constant value on the DMA for a run the stresses applied by the machine are varied to keep the strain at the set value.) This small reduction in the strain rate does not effect the results enough to prevent the comparison of the data from runs of slightly different strain setpoints.

5.0 Morphology of MCC polymers

Knowledge of the morphology of MCC family of polymers is very important for understanding the mechanical properties and interpreting the DMA data. Even though this analysis was not the focus of my study, it is necessary to use results from this portion of the study to reach conclusions from the DMA data. Therefore, I have included several pages explaining the morphology of MCC family polymers, as determined from scanning electron microscope study (SEM) at W & L.[66]

The ASTM dogbones that were prepared from the various MCC polymers (see sections 2.3 and 2.5) were fractured at the temperature of liquid nitrogen. Surfaces were produced both parallel and perpendicular to the direction of flow in the mold cavity. The parallel and perpendicular orientations mentioned here are the same as the parallel and perpendicular orientations defined in the sample preparation section, so it might be helpful to review that section here (section 4.1) and to refer to figure

9 which shows the parallel and perpendicular directions on an ASTM dogbone. Some samples were then leached with various chemicals to remove one or more of the components, and allow various features of the structures to be seen more easily. After the leaching, the fracture surfaces were gold coated and then examined with an ISI-40 SEM.[67]

The most obvious morphological feature in these materials is the presence of a complex skin/core morphology. There are three distinct regions present in all blends, even the uncompatibilized ones. There is a distinct outer skin, bordered by a strongly lamellar or intermediate layer, which is then bordered by an inner region or core. (See figure 3) The layers for the perpendicular samples are always much thinner than the layers for the parallel samples. This size difference is present in all of the different blends. For example, in the perpendicular samples both the outer and intermediate layers are around 1 to 200 microns thick, while in the parallel pieces the same layers are around 500 to 1000 microns thick. In general, the measurements of the thicknesses of the various layers seemed to be fairly similar. After the study of 5 to 10 fracture surfaces for each formulation of MCC, there was found to be a variation of up to 50%. However, there was one formulation, MCC-10SI-A, where it was very hard to determine the thickness of the various regions. The fracture surface of MCC-10SI-A appeared to be more homogeneous than the fracture surface for any other formulation. (See figure 11) In order to better define the location of the

various polymeric components of MCC, several types of chemical leaching were preformed.[68]

In the first type of leach, the fracture surfaces of all samples were suspended in toluene for two hours to extract the PS, and, after vacuum drying, were studied with the SEM. Comparing the leached and unleached surfaces of MCC-A, MCC-SI-A, and MCC-SEBSX-A revealed the PS encapsulated the PET plates and particles. (Figures 12 and 13) Analysis by infrared spectroscopy of films cast from the leaching further supports this hypothesis. In addition to encapsulating the PET, the PS formed numerous drawn fibers with draw ratios of near 10:1 in the core and 25:1 near the surface. The typical cross sections for the PS fibers ranged from 0.1 to 0.5 microns, with most fibers closer in size to the smaller value.[69]

To better determine the distribution of PET in the polyolefin matrix, samples were suspended in (1:1 volume) solution of phenol and 1,1,2,2 tetrachloroethane for 48 hours. After the samples were vacuum dried for 24 hours, they were gold coated and studied with the SEM. Although this leaching technique removes the PS, a comparison with the toluene leached samples provides a good picture of the morphology of the PET phase. The outer skin appears as a polyolefin matrix with a uniform distribution of rods and plates of PET. The intermediate layer is characterized by a strongly lamellar region that frequently appears to run cocontinously with the PE. (Figure 14) Visual inspection of numerous micrographs indicates that PET's

relative abundance appears to increase in the intermediate layer. The core region appears as a polyolefin matrix containing slightly oriented, discrete particles of PET with an aspect ratio of approximately 4:1 and ranging from 2 to 10 microns in diameter for the compatibilized blends (Figure 15) and from 5 to 15 microns for the uncompatibilized blends. As the percentage of compatibilizer increases, the particles become more uniform in size and distribution, and smaller in size.[70]

6.0 DMA of MCC polymers

The purpose of this study is to obtain information on the relative effectiveness of the compatibilizers used in the different MCC blends. One major question resulting from the original mechanical tests on the MCC family polymers, was what caused the huge difference in impact strength between the notched and unnotched impact samples. (See section 2.5) The various compatibilizers only improved the results for the unnotched impact tests. The DMA7 was used to study the distribution of the compatibilizers in the skin/core morphology. The skin was studied by running the parallel outside pieces (section 4.2.1), and the core was studied using parallel core pieces (section 4.2.2). The parallel outside pieces contained the full skin from the top and the bottom of the dogbone, and a portion of the skin from one side. The parallel core pieces contained no skin or intermediate layers, just the core.[71]

Other studies have shown that the small sample sizes of the DMA are useful for the study of the variations of properties

through out a material. The example of the skin/core morphology of polymers has been specifically mentioned as a good use of DMA.[72] It is also stated that the effects of a copolymer (compatibilizer) can be studied with the DMA.[73] This study includes both of these types of analysis.

The difference of the impact strengths could be interpreted to mean the compatibilizer is more concentrated in the skin of the molded samples. However, from studying the DMA7 curves it is possible to see that the compatibilizer appears equally in the skin and in the core. It is very evident from the DMA7 curves of the skin and core samples of MCC-10SEBSX-A and MCC-10SI-A that there is at least as much compatibilizer in the core as in the skin. For the MCC-10SI-A samples, the DMA curves for core and skin are almost identical (see figure 16), the only appreciable difference is a high temperature shift of the transitions of the PE component. The curves for MCC-10SI-A skin and core samples shows the characteristics of the glass transition in this region. Glass transitions are characterized by drastic drops in the storage modulus[74]; which is definitely the case for the -70 to -50 °C region of MCC-10SI polymers. This feature is not present in the curves of MCC, HDPE, and PET studied earlier, therefore this new peak in the loss modulus and drop in the storage modulus must be due to the compatibilizer. The shift occurs in the γ-transition region (-125 to 120°C) and the α-relaxation (40 to 60°C). The large, distinct peak in the -70 to -50 °C is the glass transition of the isoprene block of the SI compatibilizer.

It exhibits the same high temperature shift that the PE transitions do. This high temperature shift may be attributed to the increased crystallinity and ordering of the core.[75]

The results for the MCC-10SEBSX-A samples are not quite as clear as the ones for the MCC-10SI-A samples. The curves for the skin and core samples are the same shape but the magnitudes are different, but they are with in 10% of each other for both the storage modulus and tan δ (See figure 17). The error is greater for the loss modulus, but with the exception of the region surrounding the HDPE γ-relaxation, the difference is less than 20%. The most important factor to notice is the shape of the curves though, the shape of the curves for both the skin and the core regions are the same. The curves for the core region also show a high temperature shift when compared with the curves for the skin region near the HDPE γ-transition, just as the curves for the SI skin and core samples do. For the loss and storage moduli and tan δ, the curves for the core sample have a greater magnitude than the curves for the skin samples, for the regions from -155 to -25 °C and 35 to 100 °C. In the region from -25 to 35 °C the loss moduli and tan δ for the skin sample have a somewhat greater magnitude.[76]

The study and analysis of these curves shows that there must be just as much compatibilizer in the core as in the skin. The reason for this is the compatibilizer peak at approximately -50 °C on the loss modulus is an equal magnitude for both the skin and the core. Note that we are just comparing the magnitude of

the small peak in this region, not the magnitude of the entire loss modulus curves. The peak in tan δ is also the same magnitude for the skin and the core samples, and the drop in the storage moduli is about the same for both the skin and the core. The conclusion that there is just as much compatibilizer int he skin as in the core holds true for all four compatibilized formulations studied, MCC-5SI-A, MCC-10SI-A, MCC-5SEBSX-A, and MCC-10SEBSX-A. Only the data for the 10% compatibilizer formulations is presented here, and the samples molded at condition B were not studied, because of the poor surface appearance, and the possible degradation of some components associated with this poor surface appearance. The samples with 5% compatibilizer show the same results, that there must be at least as much compatibilizer in the core as in the skin.[77]

Another important comparison to make is between the various types of skin samples. The first comparison that we will make is between the MCC-A, MCC-5SI-A, MCC-5SEBSX-A samples. (See figure 18) The first feature to study is the sharp peak in the MCC-5SI-A loss modulus curve at approximately -60 °C. As stated earlier, this peak is from the glass transition of the isoprene block of the SI elastomer. The transition is also evident as a peak in tan δ, and a sharp drop in the storage modulus, but it is the most obvious in the loss modulus. The transition is also evident in the MCC-5SEBSX-A loss modulus curve, but it is in the much subtler form of a knee in the curve. It is barely noticeable in the storage modulus and tan δ, and would not be recognized unless

it was specifically looked for. In general, the glass transition is much greater in magnitude and much more well-defined in the SI samples. The curves are remarkably similar in shape with the exception of the glass transition for the SI and SEBSX compatibilizers, and a shift in the low spot of the valley of the loss moduli in the -25 to 25 °C region. The appearance of this well defined of a peak in the SI curve for a sample with only 5% of the compatibilizer suggest that the compatibilizer must be located at the interface of PET and PE, which results in much better interfacial adhesion between these two components of MCC. There may also be a small high temperature shift in the PET β-transition, which is located near the SI elastomer transition, the transition appears to be shifted to a slightly higher temperature which is closer to the SI elastomer glass transition. The SEBSX transition is less pronounced in this region when compared to the SI transition.[78]

It is also important to analyze the data for the three main sample formulations molded at the B condition, MCC-B, MCC-SI-B, and MCC-SEBSX-B. These formulations were not studied in the depth that the samples molded at condition A were, for reasons listed before. Nevertheless, it is important to at least treat them briefly in this analysis. Figure 19 shows the loss and storage moduli for the skin samples of MCC-B, MCC-5SI-B, and MCC-5SEBSX-B. The conclusions that can be reached from studying these curves are much the same as those that were reached from studying the corresponding condition A curves, so I will not give

any detailed explanation here. I will mention that for this case
the glass transition of the isoprene block is very obvious in the
MCC-5SI-B formulation, while it is barely obvious in the MCC-
5SEBSX-B sample. (At this point, the reader should be able to
verify this fact on his or her own by carefully looking at the
region form -100 to -25 °C.) The most important fact to notice
is the remarkable similarity of the curves of the samples molded
at condition B when compared with the samples molded at condition
A. This similarity should not be surprising considering that the
samples molded at both conditions are made out of the same
components. The samples molded at condition A had much better
surface appearance, and were heated to a higher temperature
before molding. These reasons caused the samples molded at
condition A t be the focus of this study, while the samples
molded at condition B were not studied in depth. The mechanical
properties of condition B samples follow the same trends as those
molded at condition A, even if the numbers are not the same.
(See section 2.5)

The next comparison to make is between the samples with 5%
and 10% of the each compatibilizer. First, a comparison of the
relative magnitudes of the isoprene block glass transition curves
for MCC-5SI-A and MCC-10SI-A (see figure 20), shows a very
distinct transition is very in both samples on all three curves,
with the magnitude about twice as great in the curves for the 10%
compatibilizer samples. The second fact to notice is that the
peak in the loss modulus in the 25 to 75 °C range is more

suppressed in the samples with 10% compatibilizer. Looking back to the comparison of all three types of samples molded under condition A is possible to see that this region is slightly suppressed in the SI sample when compared with the SEBSX and unmodified samples. This suppression of the peak becomes much greater as the amount of compatibilizer in the sample is increased. It should also be noted that after the glass transition of the isoprene block, the magnitude of the storage modulus of the 10SI sample becomes notably diminished when compared to the 5SI sample , while they where almost identical before this point. The opposite is the case for tan δ, the magnitude of tan δ increases for 10SI samples when compared to 5SI samples after the glass transition of the compatibilizer. This fact indicates that there is an increase in molecular friction due to the freeing of the isoprene block at the interface.

It is important to study the changes between curves of samples made with different percentages of the same compatibilizer to see how much difference increasing the amount of the compatibilizer makes. It is very easy to tell that a small increase in the amount of the SI compatibilizer makes a big difference in the properties. This conclusion is supported by the various mechanical properties obtained early in this study.

There are several sets of numbers that support the conclusion reached from the DMA7 data that the properties of the polymer sample can be altered dramatically by adding a small

amount of the elastomer. For example, the unnotched impact
strength of MCC-A is 128 J/m, while it is 374 J/m for MCC-5SI-A,
and the sample did not break for MCC-10SI-A. The numbers for the
stress at break and stress at yield also show the same trend as
the impact test, indicating that the mechanical properties are
very dependent upon the amount of the compatibilizer present.
The values for both of these properties consistently decrease as
the amount of compatibilizer increases. This data is exactly as
expected, because the purpose of the compatibilizer is to make
the sample less brittle (i.e. reduce the modulus) and make it
more resilient. This corresponds to the data obtained for both
the storage modulus above the temperature of the glass transition
of the isoprene block of the SI compatibilizer. Thus, there are
other results that support the conclusion that the addition of a
very small amount of the SI compatibilizer can drastically alter
the properties of the material.

Turning to the MCC-5SEBSX-A and MCC-10SEBSX-A curves (see
figure 21), we note the appearance of a small, distinct peak at
about -45 °C for both the loss modulus and tan δ in the MCC-
10SEBSX-A sample. The DMA7 curves for these two samples are very
close together and look very similar except for the appearance of
the new bump in the MCC-10SEBSX-A loss modulus and tan δ.
However, the glass transition peaks for the SEBSX elastomer are
not nearly as large distinct as the peaks for the SI elastomer.
It is also important to note that MCC-5SEBSX-A has higher loss
and storage moduli than MCC-10SEBSX-A, which is as expected,

because of the increase in the percentage of compatibilizer in the sample. The mechanical properties did not improve as much from the addition of the SEBSX compatibilizer as from the addition of the SI compatibilizer, which might be expected from the relative similarity of the curves in figure 21. The SEBSX elastomer does not increase the impact strength nearly as much as the SI elastomer and the increase between samples with 5% and 10% is not as great either. The relative ineffectiveness of increasing the amount of the SEBSX elastomer may also be seen by comparing many other values in section 2.5. Thus, the similarity of the DMA7 curves for samples prepared with 5% and 10% of the SEBSX elastomer suggests that increasing the amount of the SEBSX compatibilizer has much less effect on the properties than increasing the amount of the SI compatibilizer, and that SI is, in general, a better compatibilizer. This conclusion is confirmed by study the mechanical property data in section 2.5.

7.0 Results

Now we consider some conclusions derived from both the DMA and SEM data. First, in the presence of the PE matrix in MCC, the PS encapsulates the particles of PET. Surface energy calculations outlined in Hobbs et al show that PS has the ability to displace the polyolefin matrix from the surface region of the PET phase.[79] Next we consider the interfacial interaction of the various compatibilizers: the styrenic part of the SI compatibilizer may be said to either attach directly to the PET, behaving like PS and encapsulating the PET, or to attaches to

both the PS and PET phases. At the same time, the isoprene block portion of the SI compatibilizer mixes with the PE portion of MCC. On the other hand, the polar groups located on the anhydride modified SEBSX compatibilizer decrease the effectiveness of this process. The implication of this fact, is that the unmodified version of this compatibilizer, called SEBS, would be a better compatibilizer for the PET component, than the modified one. This conclusion is based on the DMA data and the mechanical test data, which both show that SEBSX is a much less effective compatibilizer than SI.[80]

ASTM test specifications for the notched Izod impact test place the tip of the notch well inside the core of the sample. The skin and intermediate layers extend, at most, 1 to 1.5 mm into the sample for perpendicular samples. From the study of the DMA curves it is known that there is just as much compatibilizer in the skin as in the core, which leads to the conclusion that the difference between the two impact strengths must be based upon morophologigal features of the samples. The presence of the drawn rods and plates of PS and PET in the skin and intermediate layer combined with the bonding between these brittle phases and the more ductile polyolefin matrix provides much more strength to absorb the energy due to impact than the features of the core. This suggests that the core, which consists of oriented, brittle particles of PET with interfacial bonding in the polyolefin matrix, is not capable of absorbing impact well. This in turn implies that, the cocontinous, interlocking morphology of the

intermediate layer, when compatibilized, forms a tough integral band of material that resists fracture upon impact. The particulate dimensions with in the core, even when bonded with the matrix, do not provide any significant improvement in impact strength in comparison with the uncompatibilized, base material.[81]

8.0 Conclusions

If processed under very specific conditions, blends of refined waste plastics consisting of recycled PE, PET, and PS in approximately the ratio of 6:3:1 by weight, produce materials with a complex skin/core morphology. These materials are typically characterized by a strongly lamellar, sometimes cocontinous, band consisting of alternating interlocking phases of PET and PE. In an unmodified form, these materials are prone to delamination and brittle fracture through out this region. Adding an effective compatibilizer in the form of an elastomer, which locates at the PET/PE interface, exploits the entangled morphology, resulting in good impact properties.[82]

One variable which has been barely touched upon, but which would influence mechanical properties, is the variation, if any, in the relative amount of PET to PE as a function of depth from the outer surface of the sample. Infrared spectroscopic studies of thin films sectioned from MCC samples are currently in progress at W & L to measure the distribution of PET through out the molded articles. As a complement to these measurements, positron annihilation is being applied, and molecular packing

density as a function of depth is calculated. This information ought to provide a through analysis and understanding of the microstructure, morphology, and mechanical behavior of these complex materials.[83]

List of Figures

by PS (dark gap around PET), which has been removed by leaching. Magnification: 5.3 kX.

Figure 14   Micrograph of fracture surface for MCC-5SI-A parallel to direction of flow, showing the lamellar co-continuous, intermediate layer, consisting of plates of PE and PET. PET plates have been removed by leaching, enhancing the effect. Magnification: 1.24 kX.

Figure 15   Micrograph of the fracture surface for MCC-10SI-A, parallel to the flow, showing the core. PET particles have been removed by leaching and appear as darkened elliptical particles with an aspect ratio of about 4:1, ranging in size from 2-10 microns. PET particles for uncompatibilized blends are less uniform in size and distribution and range in size from 5-15 microns. Magnification: 1.2 kX.

Figure 16   DMA7 curves for MCC-10SI-A skin and core samples.

Figure 17   DMA7 curves for MCC-10SEBSX-A skin and core samples.

Figure 18   DMA7 curves for the skin samples of MCC-A, MCC-5SEBSX-A, and MCC-10SI-A. The glass transition of the isoprene block of the SI elastomer, -70 to -50 °C) is very well defined for only 5% of the elastomer, suggesting enhanced interfacial adhesion at the PET/PE interface. The transition is much less pronounced for MCC-5SEBSX-A.

Figure 19   DMA7 curves for the skin samples of MCC-B, MCC-5SEBSX-B, and MCC-5SI-B.

Figure 20   DMA7 curves for the skin samples of MCC-5SI-A and MCC-10SI-A.

Figure 21   DMA7 curves for the skin samples of MCC-5SEBSX-A and MCC-10SEBSX-A.

References

1. Richard W. Renfree, <u>Mechanical and Physical Properties of Recycled, Commingled, Polymeric Materials</u>, Center for Plastics Recycling Research, NJ (1991) 1.

2. Thomas D. Traugott, <u>Mechanical Properties and Morphologies of HDPE-PET Blends</u>, University of Texas at Austin (1982) 1.

3. Renfree 1-2.

4. Traugott 1.

5. Renfree 7.

6. Renfree 7.

7. M. Xanthos et al., <u>Compatibilization of Refined Commingled Post-Consumer Plastics</u>, Society of Plastics Engineers Annual Technical Conference 1992 (1992) 596.

8. D.R. Paul and J.W. Barlow, "Polymer Blends (or Alloys)", <u>Journal of Macromolecular Science - Review of Macromolecular Chemistry</u>, (New York: M. Dekker, 1980) 110.

9. D.R. Paul and J.W. Barlow, "Polymer Blends (or Alloys)" 110-111.

10. D.R. Paul and J.W. Barlow, "Polymer Blends (or Alloys)" 111-112.

11. D.R. Paul and J.W. Barlow, "Polymer Blends (or Alloys)" 112.

12. J.W. Barlow and D.R. Paul, "Polymer Blends and Alloys - A Review of Selected Considerations", <u>Polymer Science and Engineering</u>, Vol. 21 No. 15 (1981) 986.

13. D.R. Paul and J.W. Barlow, "Polymer Blends (or Alloys)" 114.

14. Xanthos et al. 596.

15. Xanthos et al. 598.

16. K.E. Van Ness et al., "Properties and Microstructure of Impact Modified Post-Consumer Plastics", Paper Number 288, <u>Society of Plastics Engineering Annual Technical Conference 1993</u> (1993).

17. Xanthos et al. 596.

18.   Van Ness et al.

19.   Traugott 11.

20.   C.A. Daniels, <u>Polymers: Structure and Properties</u> (Lancaster: Technomic Publishing, 1989) 74-75.

21.   Traugott 11.

22.   Traugott 9-10.

23.   Daniels 72-73.

24.   Elizabeth Dale Wyatt, <u>Scanning Electron Microscopy Studies of Recycled Polystyrene/Polyolefin Blends</u>, (Lexington, VA: Senior Thesis, Washington and Lee University, 1992) 5.

25.   Daniels 52.

26.   Xanthos et al. 596.

27.   Van Ness et al.

28.   Xanthos et al. 596-597.

29.   Xanthos et al. 599.

30.   Van Ness et al.

31.   Xanthos et al. 597.

32.   Van Ness et al.

33.   Xanthos et al. 597-599.

34.   Xanthos et al. 599.

35.   Xanthos et al. 597-599.

36.   Xanthos et al. 597-599.

37.   Xanthos et al. 597-599.

38.   Xanthos et al. 597-599.

39.   Xanthos et al. 597-599.

40.   Xanthos et al. 597-599.

41.   N.G. McCrum, B.E. Read, and G. Williams, <u>Anelastic and Dielectric Effects in Polymeric Solids</u> (New York: Dover Publications, 1967) 192, 195, 197, 200.

42. McCrum, Read, and Williams 192-194.

43. McCrum, Read, and Williams 195-196.

44. McCrum, Read, and Williams 195.

45. McCrum, Read, and Williams 195-196.

46. McCrum, Read, and Williams 197-199.

47. McCrum, Read, and Williams 200.

48. Stephen L. Rosen, <u>Fundamental Principles of Polymeric Materials</u> (New York: John Wiley and Sons, 1982) 256-257.

49. Rosen 257-259.

50. "DMA7 Dynamic Mechanical Analyzer", <u>The Perkin Elmer 7 Series Thermal Analysis System</u> (Norwalk, CT: Perkin Elmer Corporartion, 1990) 6-1 through 6-6.

51. Takayuki Murayama, <u>Dynamic Mechanical Analysis of Polymeric Material</u> (Amsterdam: Elsevier Scientific Publishing, 1978) 2.

52. Murayama 10-11.

53. Murayama 13-17.

54. Murayama 61-64.

55. McCrum, Read, and Williams 357.

56. McCrum, Read, and Williams 358.

57. McCrum, Read, and Williams 361.

58. McCrum, Read, and Williams 366.

59. McCrum, Read, and Williams 371.

60. McCrum, Read, and Williams 501.

61. McCrum, Read, and Williams 504-506.

62. McCrum, Read, and Williams 517-520.

63. McCrum, Read, and Williams 409-414.

64. McCrum, Read, and Williams 377-380.

65. D. Campbell and J.R. White, <u>Polymer Characterization - Physical Techniques</u> (New York: Chapman and Hall, 1989) 320.

66. Van Ness et al.

67. Van Ness et al.

68. Van Ness et al.

69. Van Ness et al.

70. Van Ness et al.

71. Van Ness et al.

72. Campbell and White 321.

73. Campbell and White 322.

74. Murayama 60-61.

75. Van Ness et al.

76. Van Ness et al.

77. Van Ness et al.

78. Van Ness et al.

79. S.Y. Hobbs, M.E.J. Dekkers, and V.H. Watkins, Polymer, 29(9) (1988) 1598.

80. Van Ness et al.

81. Van Ness et al.

82. Van Ness et al.

83. Van Ness et al.

Bibliography

Perkin Elmer Corporation. "Dynamic Mechanical Analyzer 7", The
    Perkin Elmer 7 Series Thermal Analysis System. Norwalk, CT:
    The Perkin Elmer Corporation, 1990.

Barlow J.W., and D.R. Paul. "Polymer Blends and Alloys - A
    Review of Selected Considerations." Polymer Science and
    Engineering Vol. 21 No. 15 (1981) 985-996.

Campbell, D. and J.R. White. Polymer Characterization -
    Physical Techniques. New York: Chapman and Hall, 1989.

Hobbs, S.Y., M.E.J. Dekkers, and V.H. Watkins. Polymer, 29(9)
    (1988) 1598.

Locke, C.E. and D.R. Paul. "Graft Copolymer Modification of
    Polyethylene Polystyrene Blends. II. Properties of Modified
    Blends." Journal of Applied Polymer Science 17 (1973):
    2791-2800.

McCrum, N.G., B.E. Read, and G. Williams. Anelastic and
    Dielectric Effects in Polymeric Solids. New York: Dover
    Publications, 1967.

Murayama, Takayuki. Dynamic Mechanical Analysis of Polymeric
    Material. Amsterdam: Elsevier Scientific Publishing, 1978.

Paul, D.R., and J.W. Barlow. "Polymer Blends (or Alloys)."
    Journal of Macromolecular Science - A Review of
    Marcomolecular Chemistry C18(1) (1980): 109-168.

Renfree, Richard W. Mechanical and Physical Properties of
    Recycled, Comingled, Polymeric Materials. New Bunswick, NJ:
    Center for Plastics Recycling Research, 1991.

Takayanagi, Motowo. "Viscoelastivc Properties of Crystalline
    Polymers." Memoirs of the Faculty of Engineering Kyushu
    University 23 (1963): 41-96.

Traugott, Thomas D. Mechanical Properties and Morphologies of
    HDPE-PET Blends. Austin: University of Texas at Autsin,
    1982.

Traugott, T.D., and J.W. Barlow, and D.R. Paul. "Mechanical
    Compatibilization of High Density Polyehtylene-Poly(ethylene
    Terephalate) Blends." Journal of Applied Polymer Science 28
    (1983): 2947-2959.

Wyatt, Elizabeth Dale. Scanning Electron Miscrocopy Studies
    of Recycled Polystyrene/Polyolefin Blends. Lexinton, VA:

Senior Thesis, Washington and Lee University, 1992.

Van Ness, K.E., et al. "Properties and Microstructure of Impact Modified Post-Consumer Plastics." Society of Plastics Engineers Annual Technical Conference Paper No. 288 (1993).

Xanthos, M., T.J. Nosker, and K.E. Van Ness. "Compatibilization for Reuse of Commingled Post-Consumer Plastics." Compalloy '92, Short Hills, NJ (1992).

Xanthos, M. et al. "Compatibiliaztion of Refined Comingled Post-Consumer Plastics." Society of Plastics Engineers Annual Technical Conference 1992 (1992) 596-601.

Gibb's Free Energy of Mixing versus the Volume Fraction of Component 2 of the Mixture
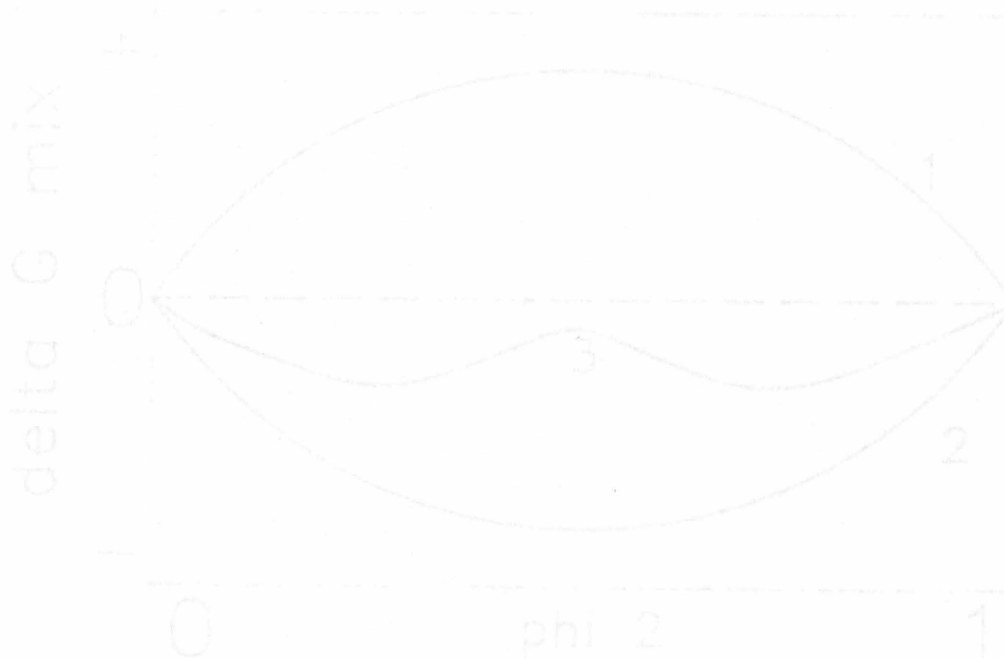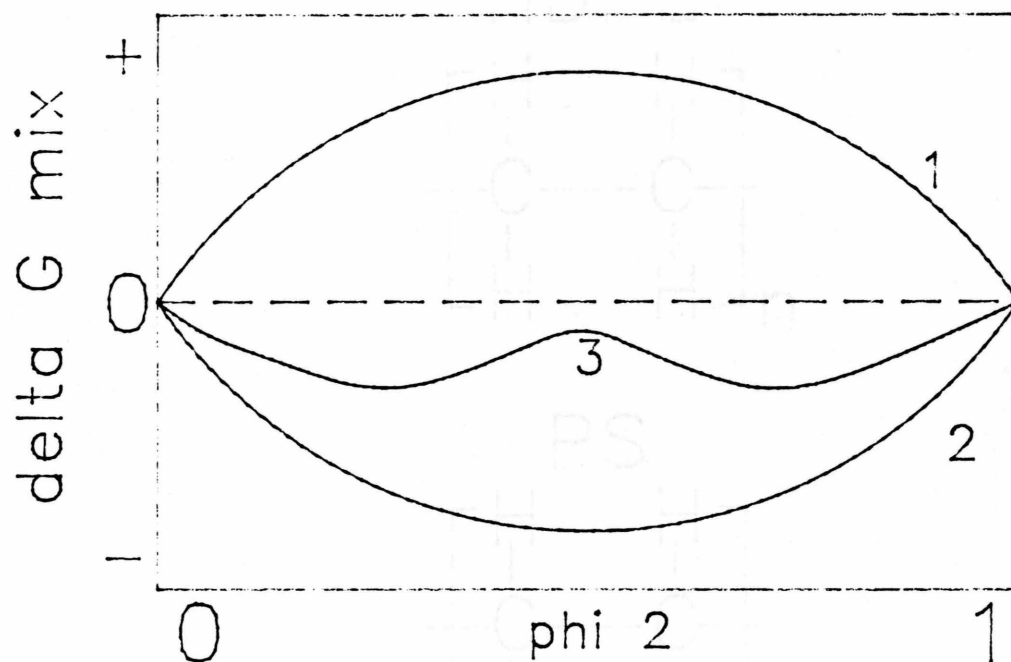
Figure 1   The Gibb's Free Energy of Mixing for a polymer blend versus the volume fraction of the second component of the blend. Curve 1 - Completely immiscible blend.   Curve 2 - Completely miscible blend.   Curve 3 - Partially miscible blend.

Figure 2   A single mer for PET, HDPE, and PS.
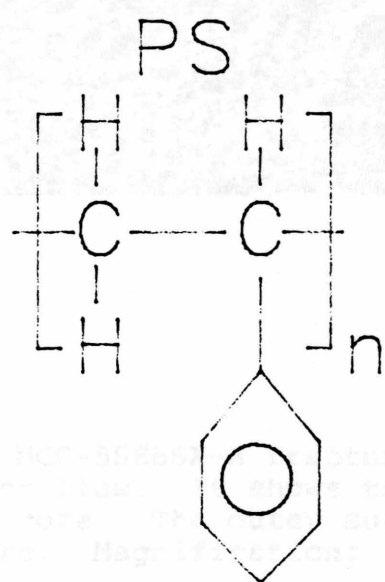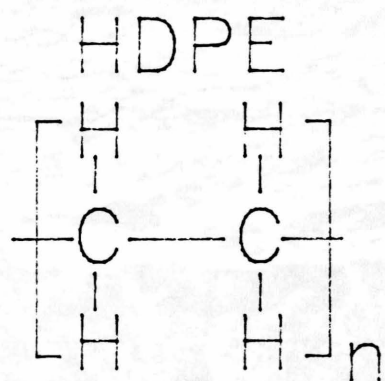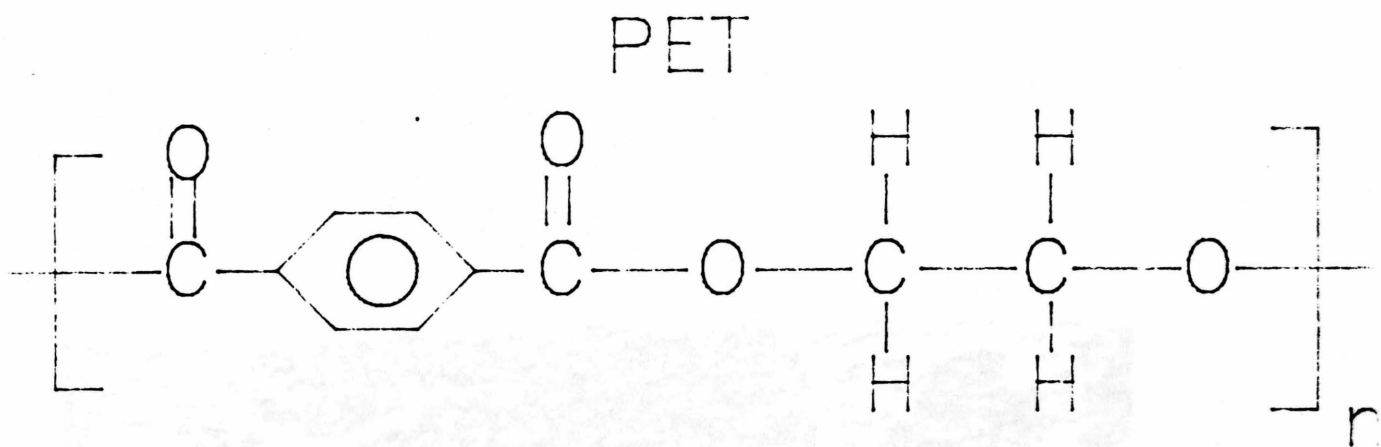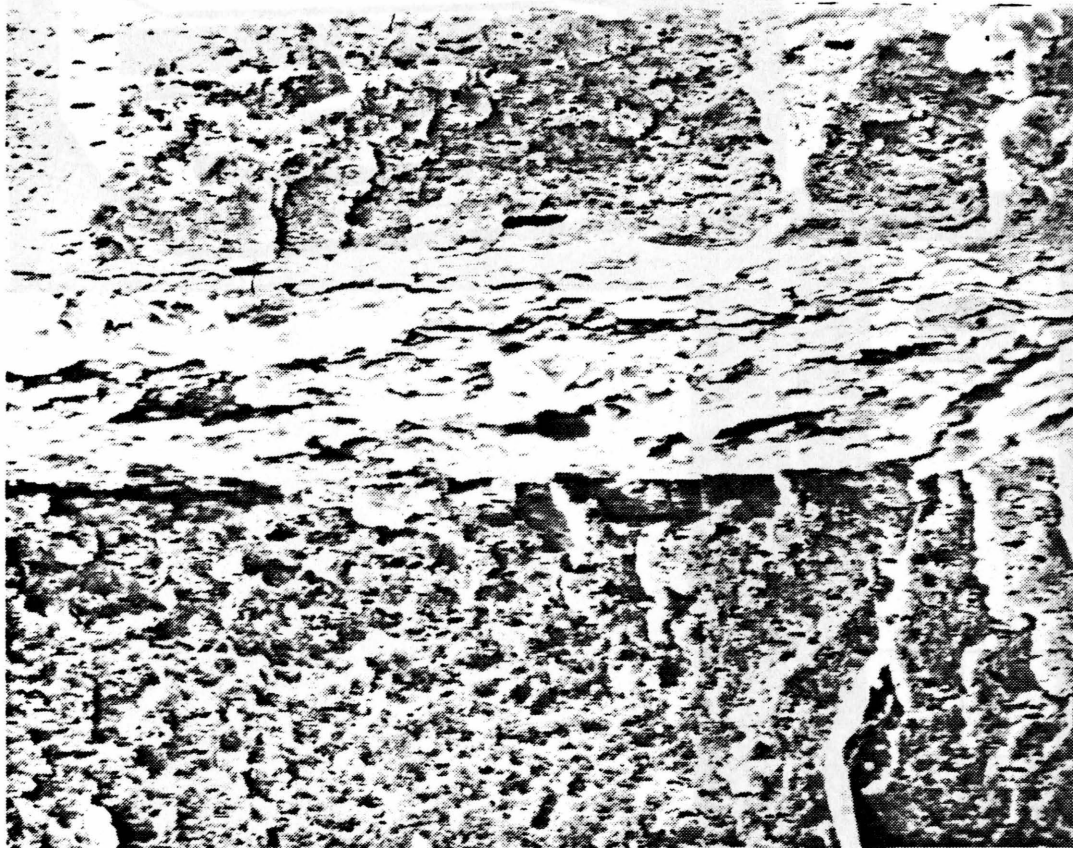
Figure 3   Micrograph of a MCC-5SEBSX-A fracture surface that is
parallel to the direction of flow.   It shows the outer skin, the
intermediate layer and the core.   The outer surface of the sample
is at the top of the picture.   Magnification: 1.2 kX.

Figure 4   The computer controlled Perkin Elmer Dynamic
Mechanical Analyzer 7 (DMA7) used in the dynamic mechanical
analysis section of this paper.
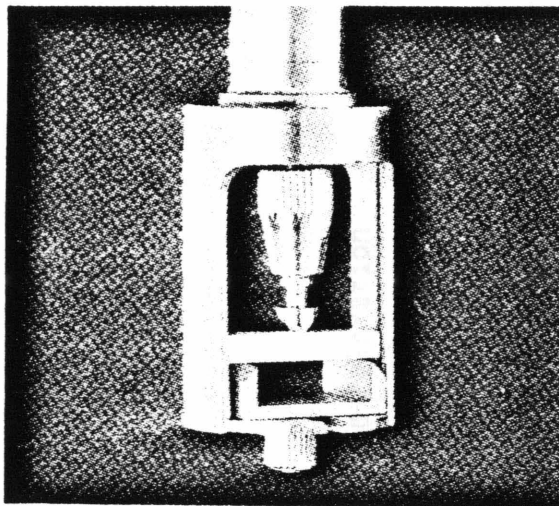
Figure 5   The three point bending measuring system for the DMA7;
the measuring system used in this study.
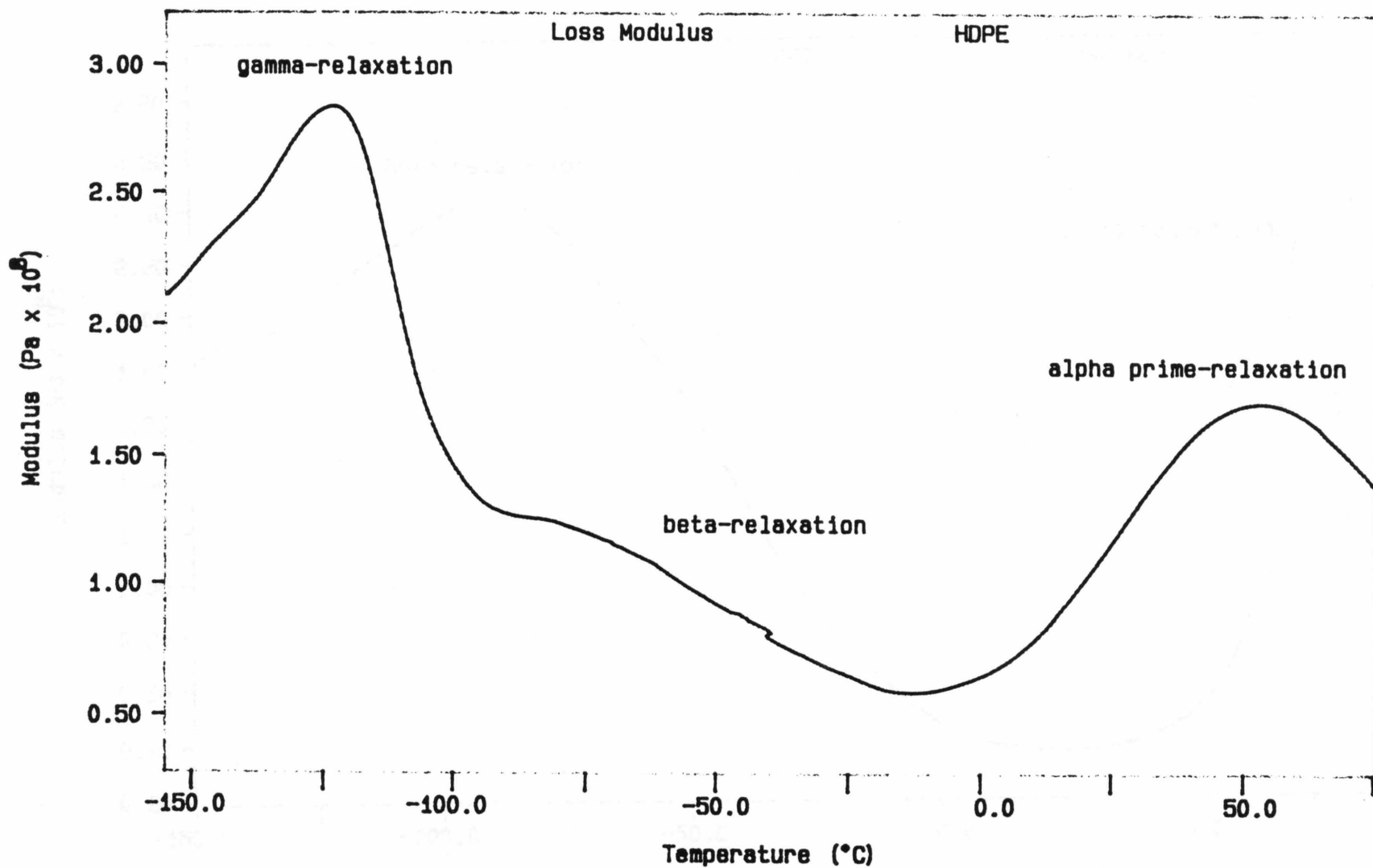
Figure 6a   The loss modulus for HDPE.   All of the major
relaxations are labeled.
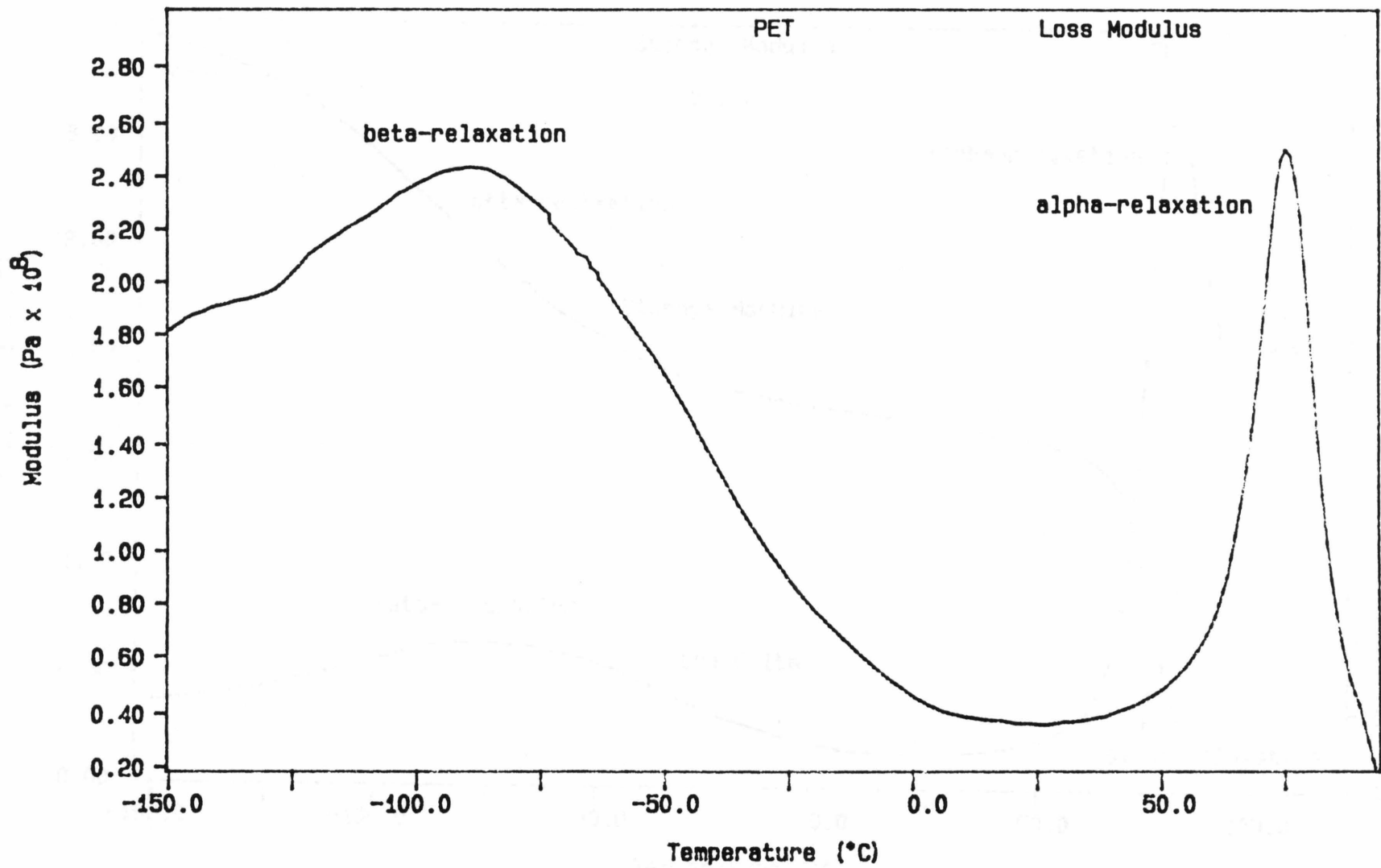
Figure 7a   The loss modulus for PET.   All of the major
relaxations are labeled.
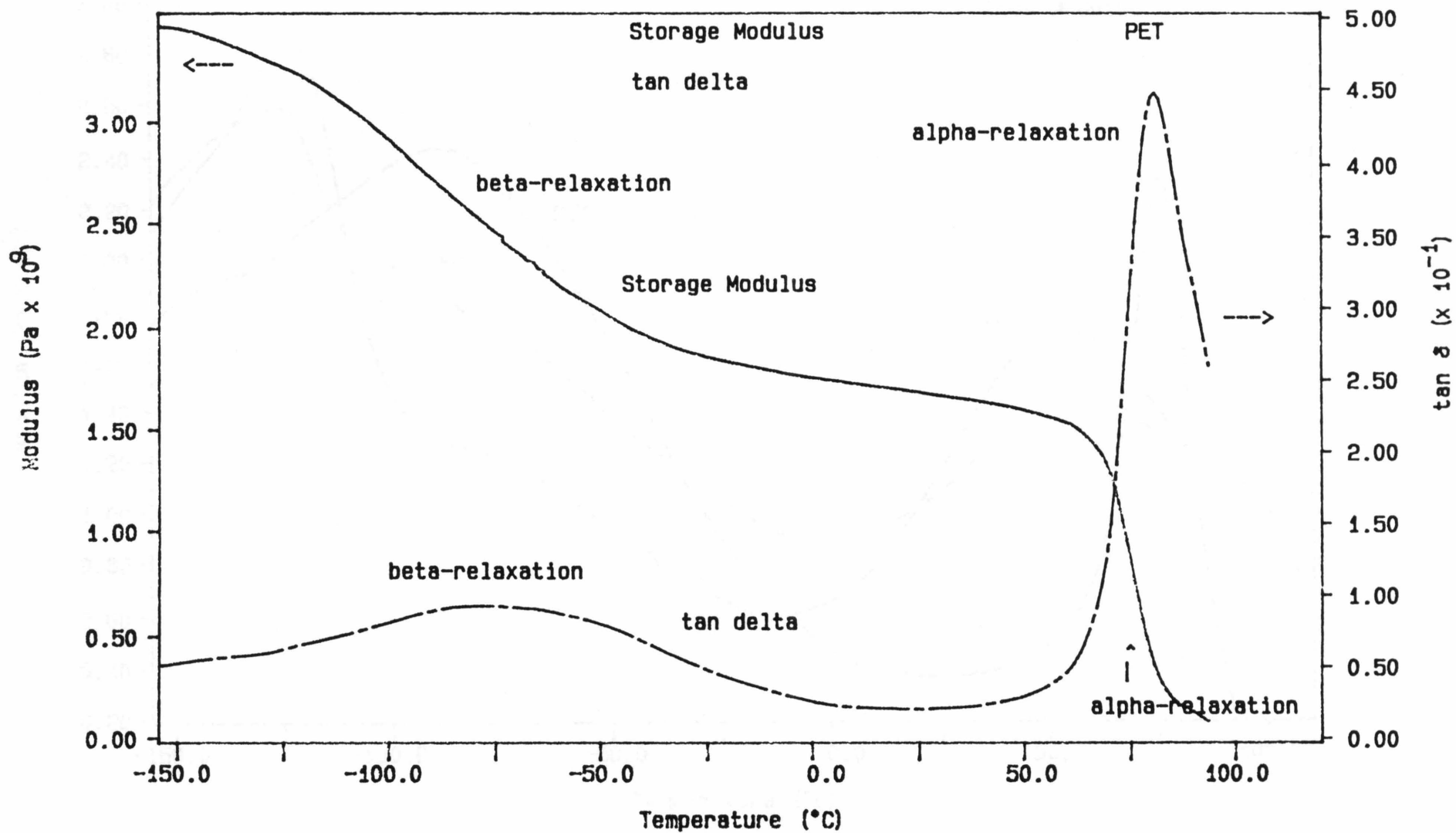
Figure 7b   The storage modulus and tan δ for PET.   All of the
major relaxations are labeled.
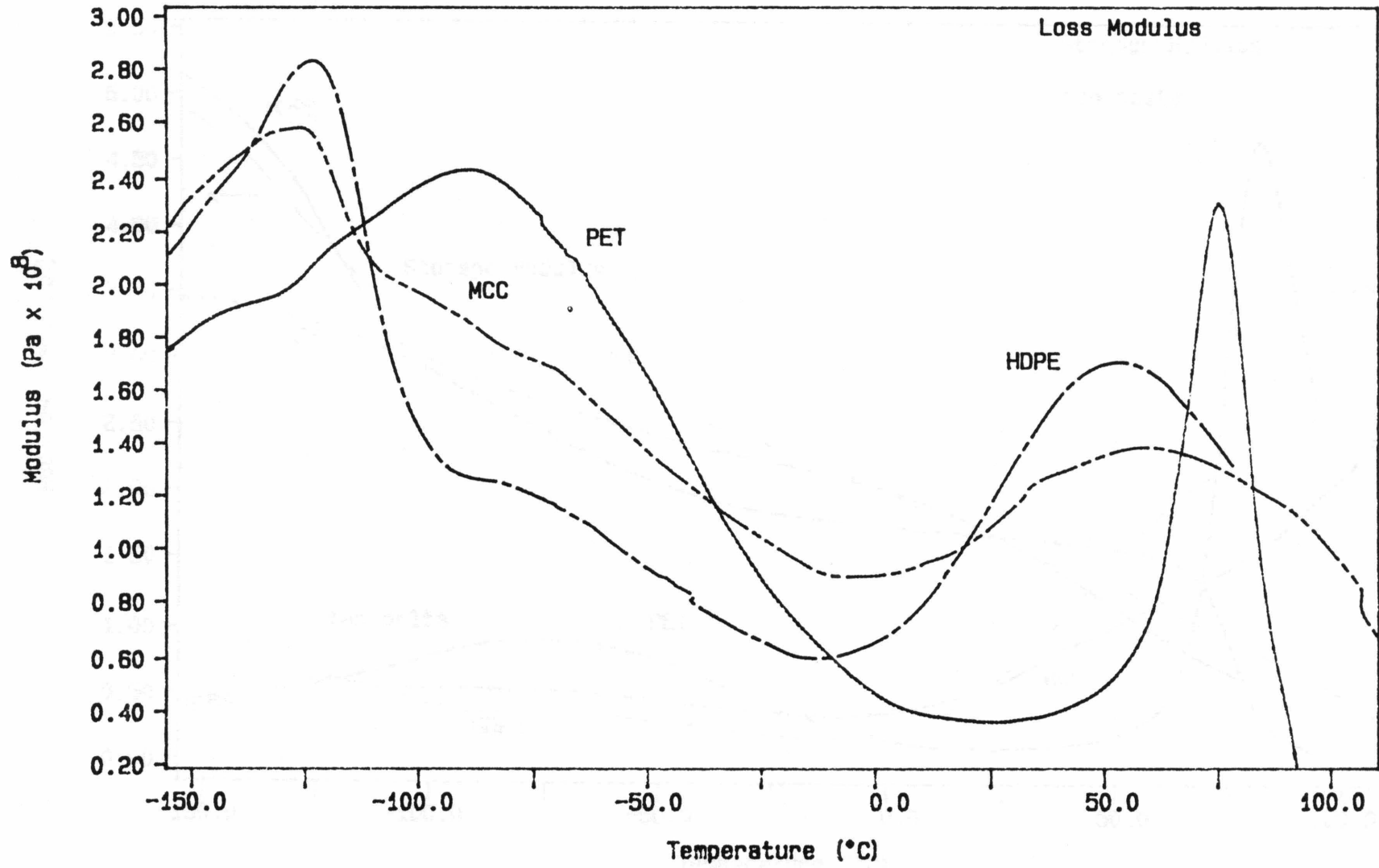
Figure 8a   The loss modulus for HDPE, PET, and an
uncompatibilized MCC family polymer.
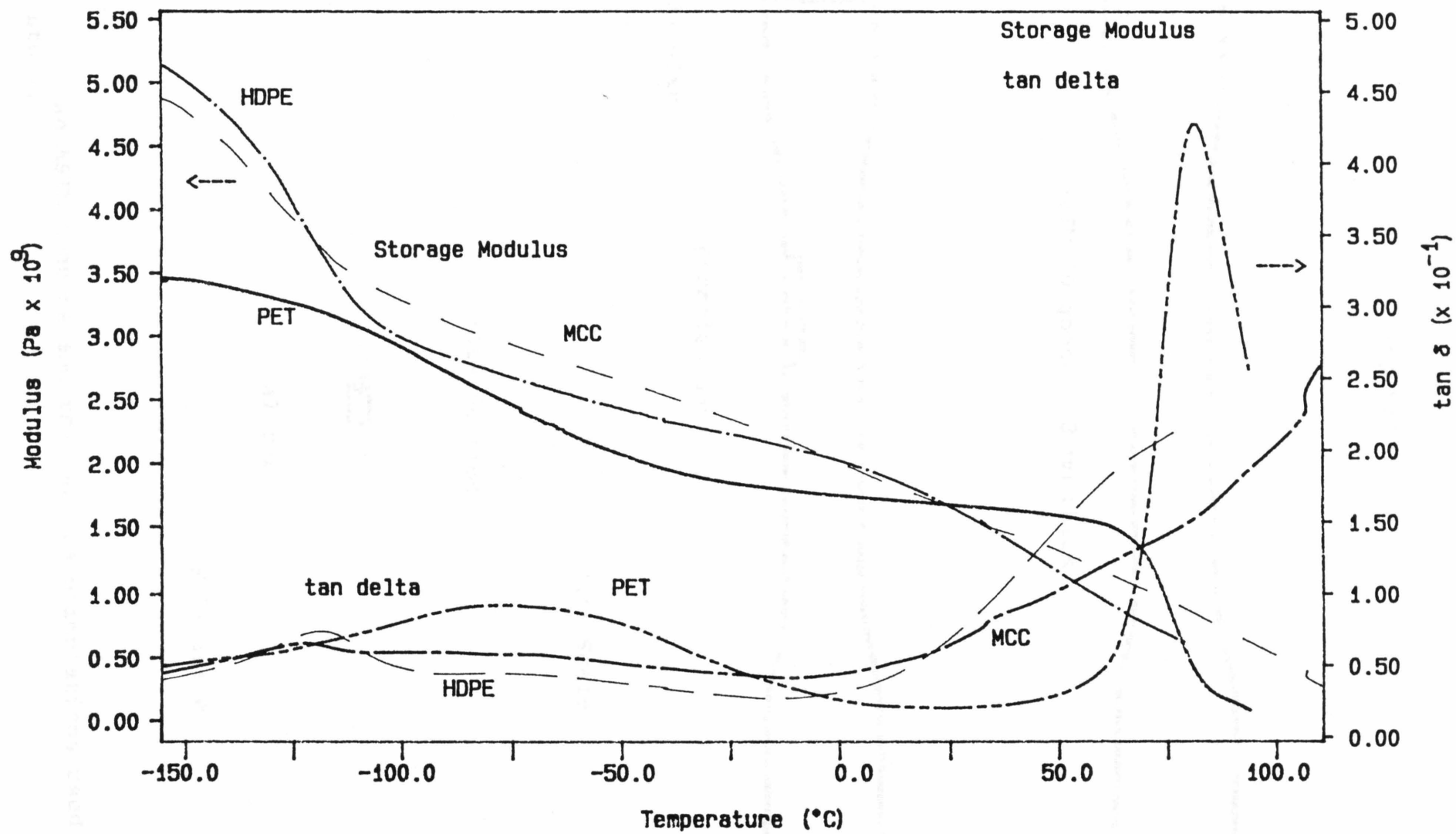
Figure 8b   The storage modulus and tan δ for HDPE, PET, and an uncompatibilized MCC family polymer.
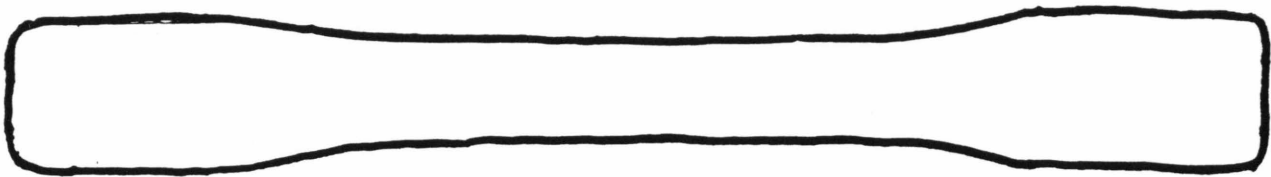
ASTM "Dogbone"   3 mm thick
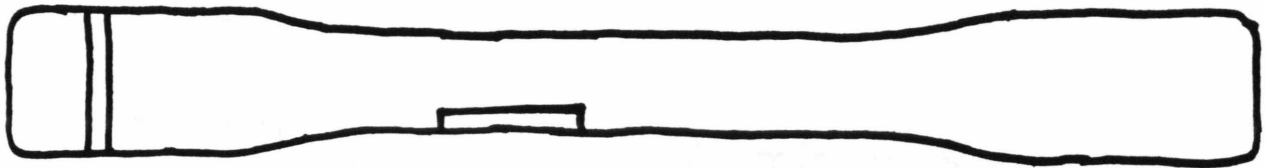
perpendicular

parallel outside

Full Scale

Cross Section

parallel core

Full Scale

Figure 9   An ASTM dogbone and the various orientations used in this study.

Set Screws

Aluminum Support

Sample

Brass Support
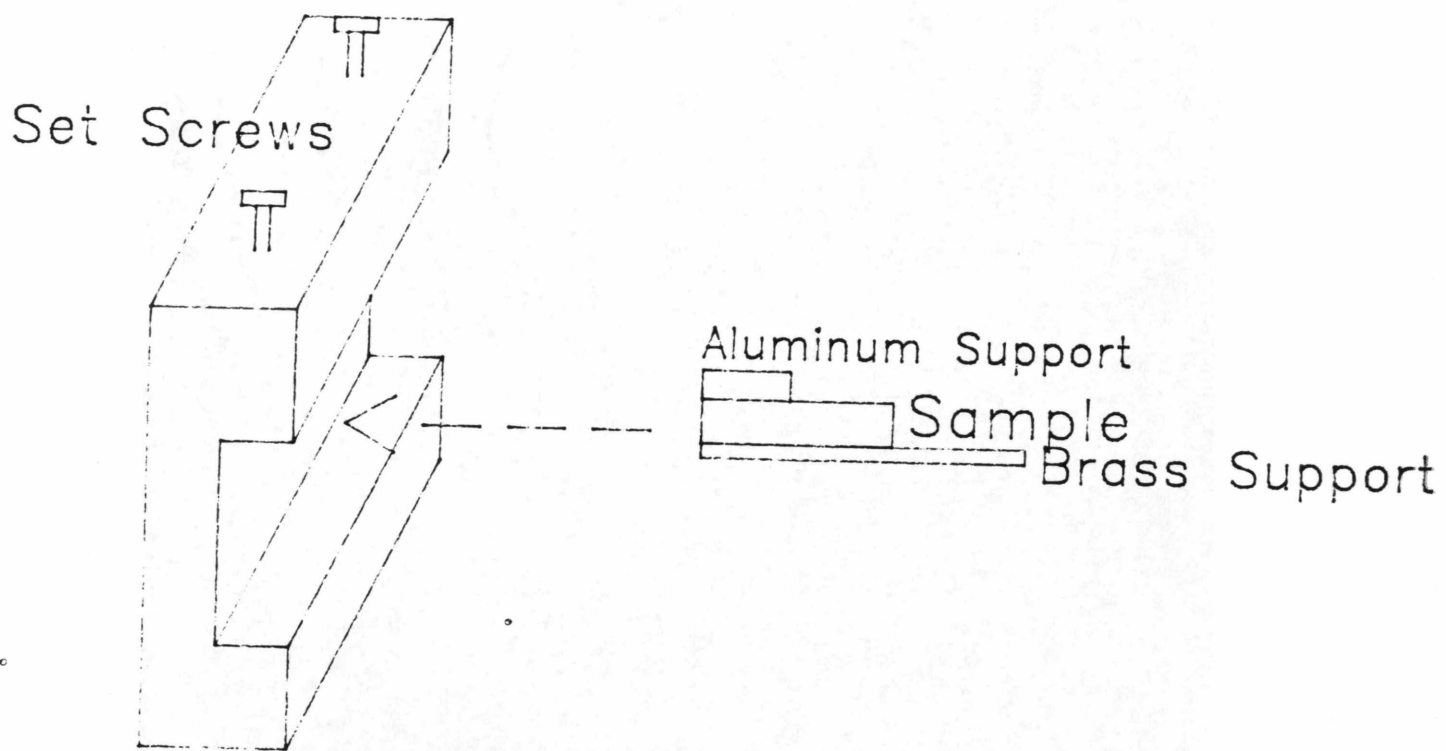
Figure 10   The "jig" used to hold the piece of the dogbone as a
parallel outside sample is prepared on the Hardinge Milling
machine.
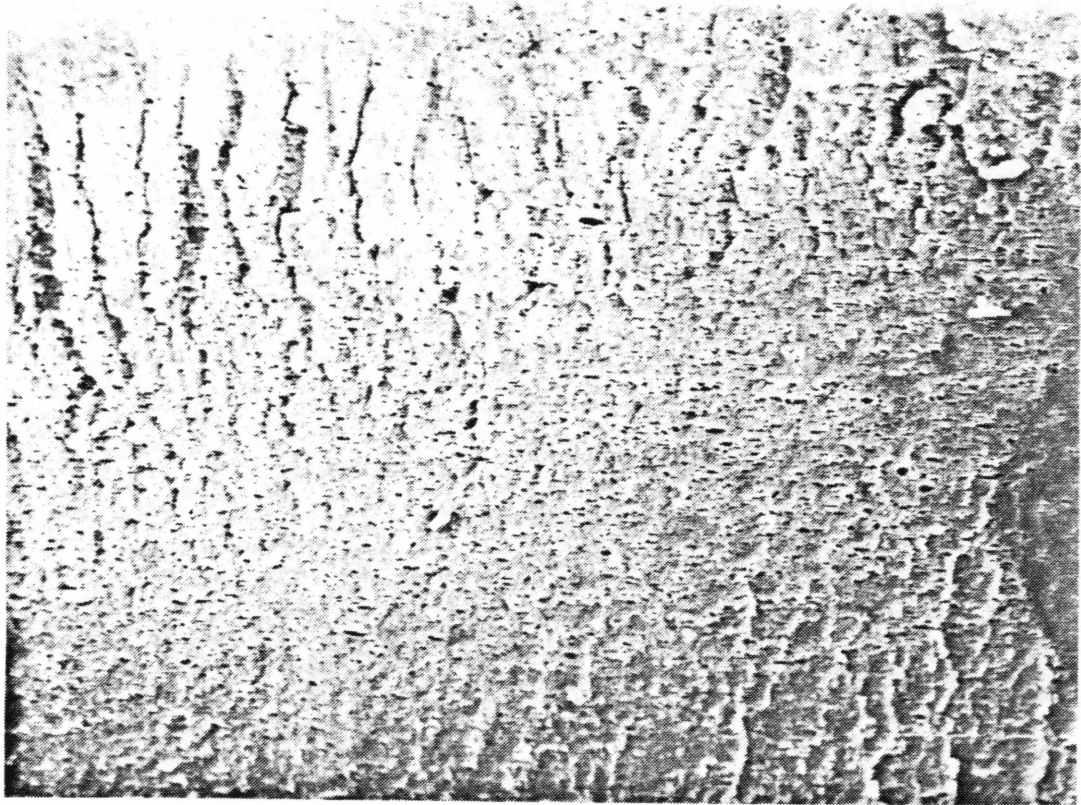
Figure 11   Micrograph of the fracture surface for MCC-10SI-A.
The three layers are much less distinct for this formulation than
for the others.   Magnification: 81 X
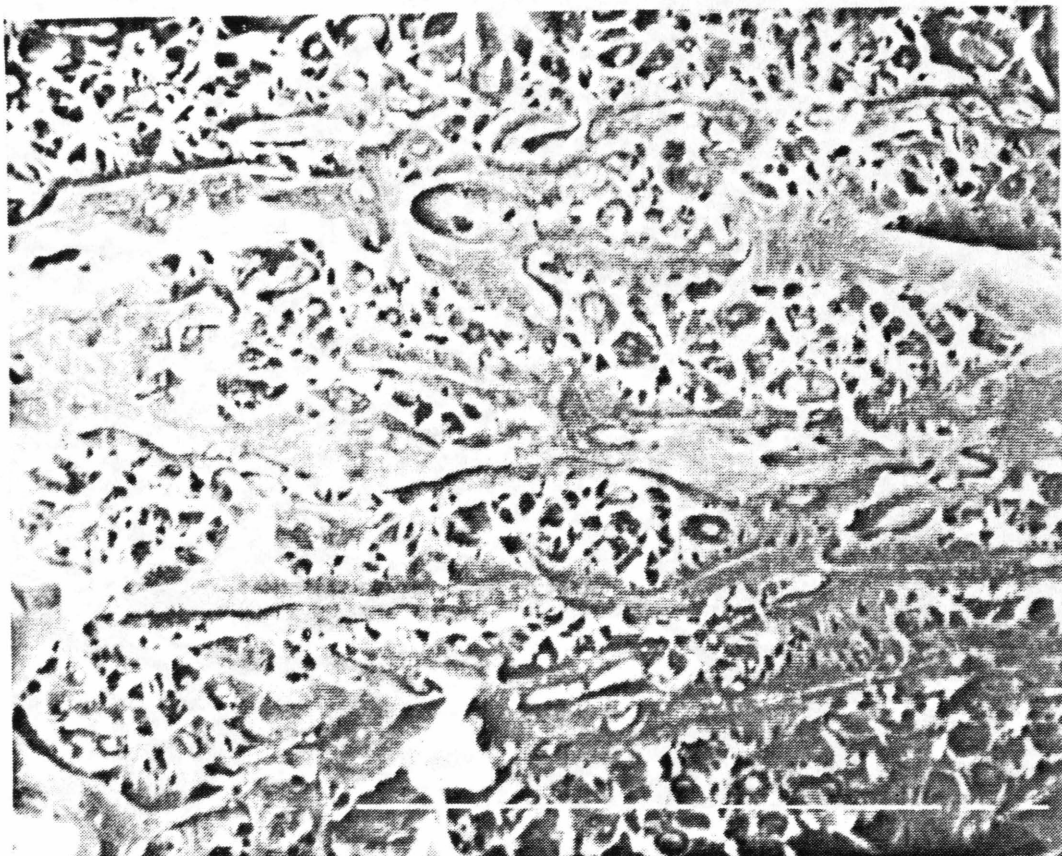
Figure 12   Micrograph of the fracture surface for MCC-5SI-A
perpendicular to the direction of flow, showing the intermediate
layer.   Smooth "fingers" of PET run concontiously through the
dimpled HDPE matrix.   No leaching was preformed on this sample.
Magnification: 5.2 kX.
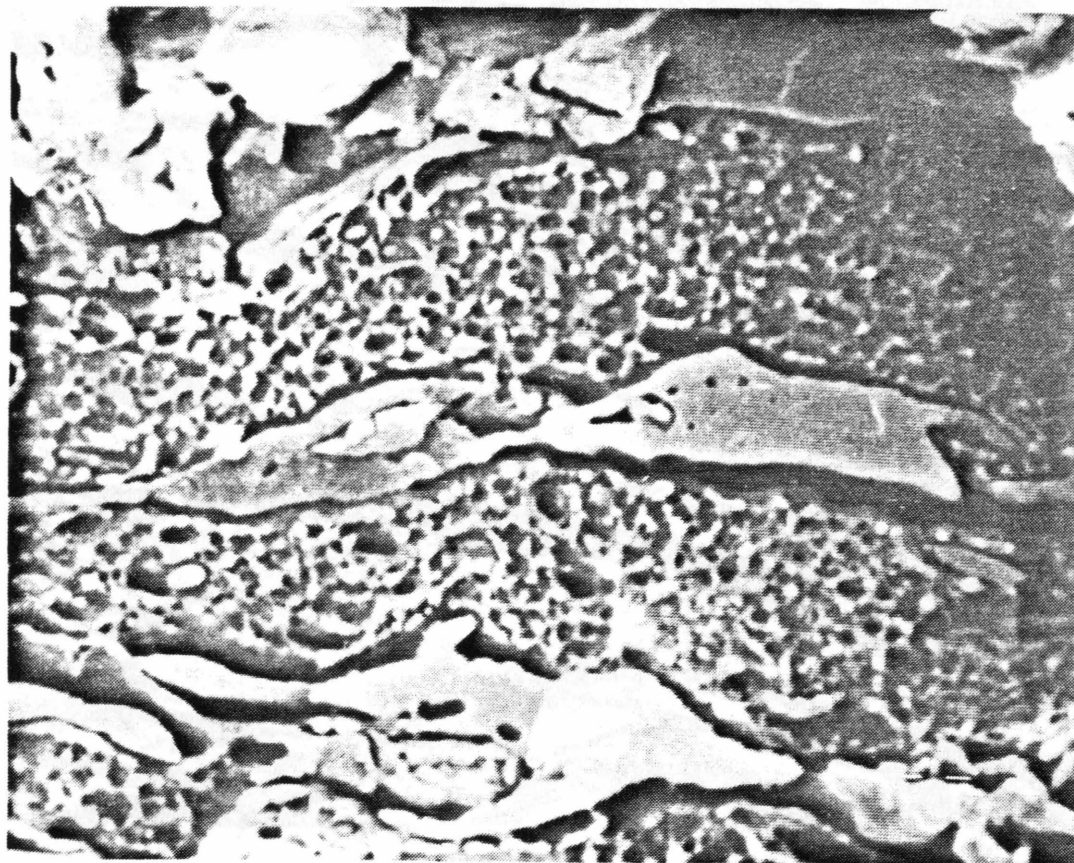
Figure 13   Micrograph of the fracture surface for MCC-5SI-A
perpendicular to the direction of flow, showing the encapsulation
of the PET phase (smooth plates in the dimpled polyolefin matrix)
by PS (dark gap around PET), which has been removed by leaching.
Magnifiaction: 5.3 kX.
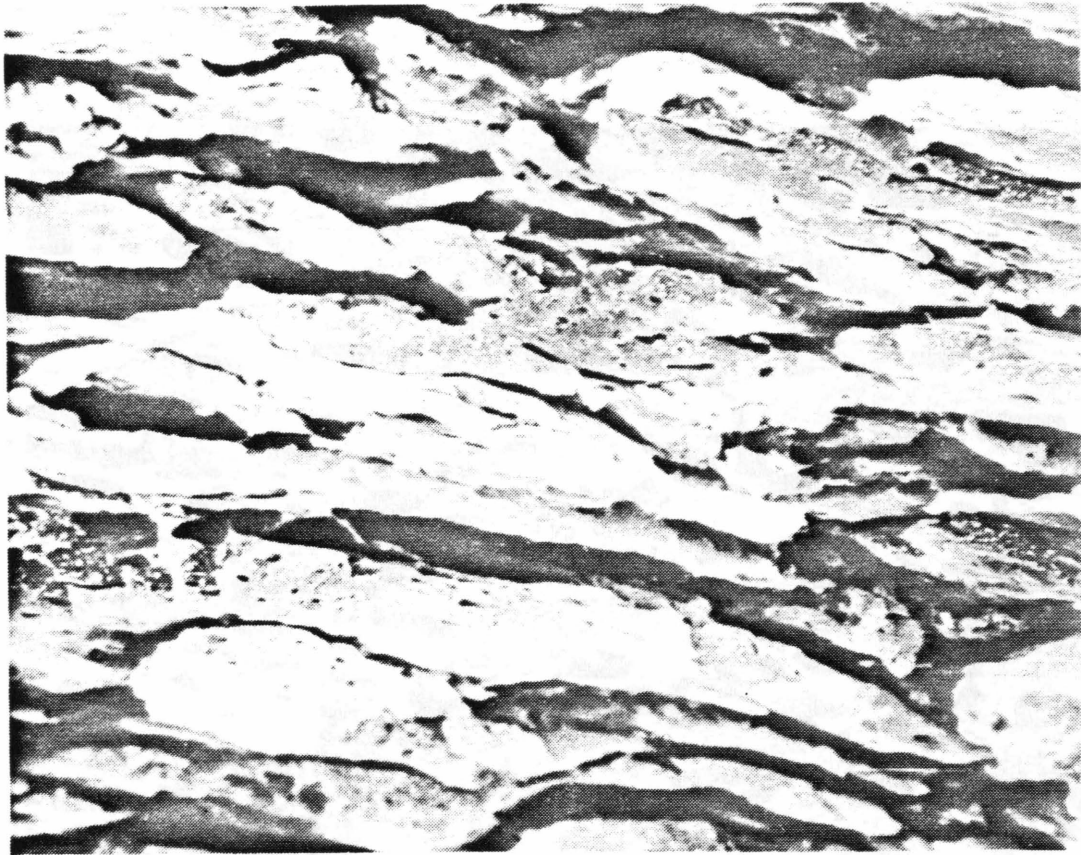
Figure 14   Micrograph of fracture surface for MCC-5SI-A parallel
to direction of flow, showing the lamellar co-continuous,
intermediate layer, consisting of plates of PE and PET.   PET
plates have been removed by leaching, enhancing the effect.
Magnification: 1.24 kX.
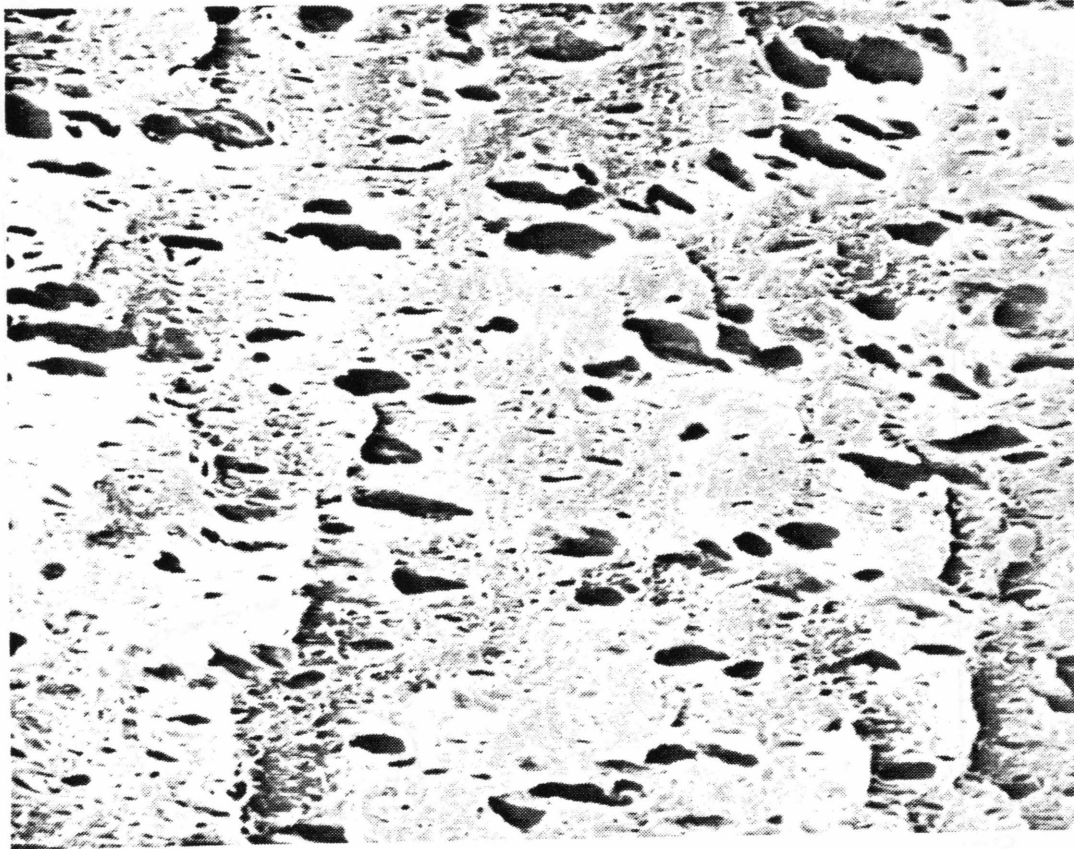
Figure 15   Micrograph of the fracture surface for MCC-10SI-A,
parallel to the flow, showing the core. PET particales have been
removed by leaching and appear as darkened elliptical particles
with an aspect ratio of about 4:1, ranging in size from 2-10
microns. PET particles for uncompatibilezed blends are less
uniform in size and distribution and range in size from 5-15
microns. Magnification: 1.2 kX.
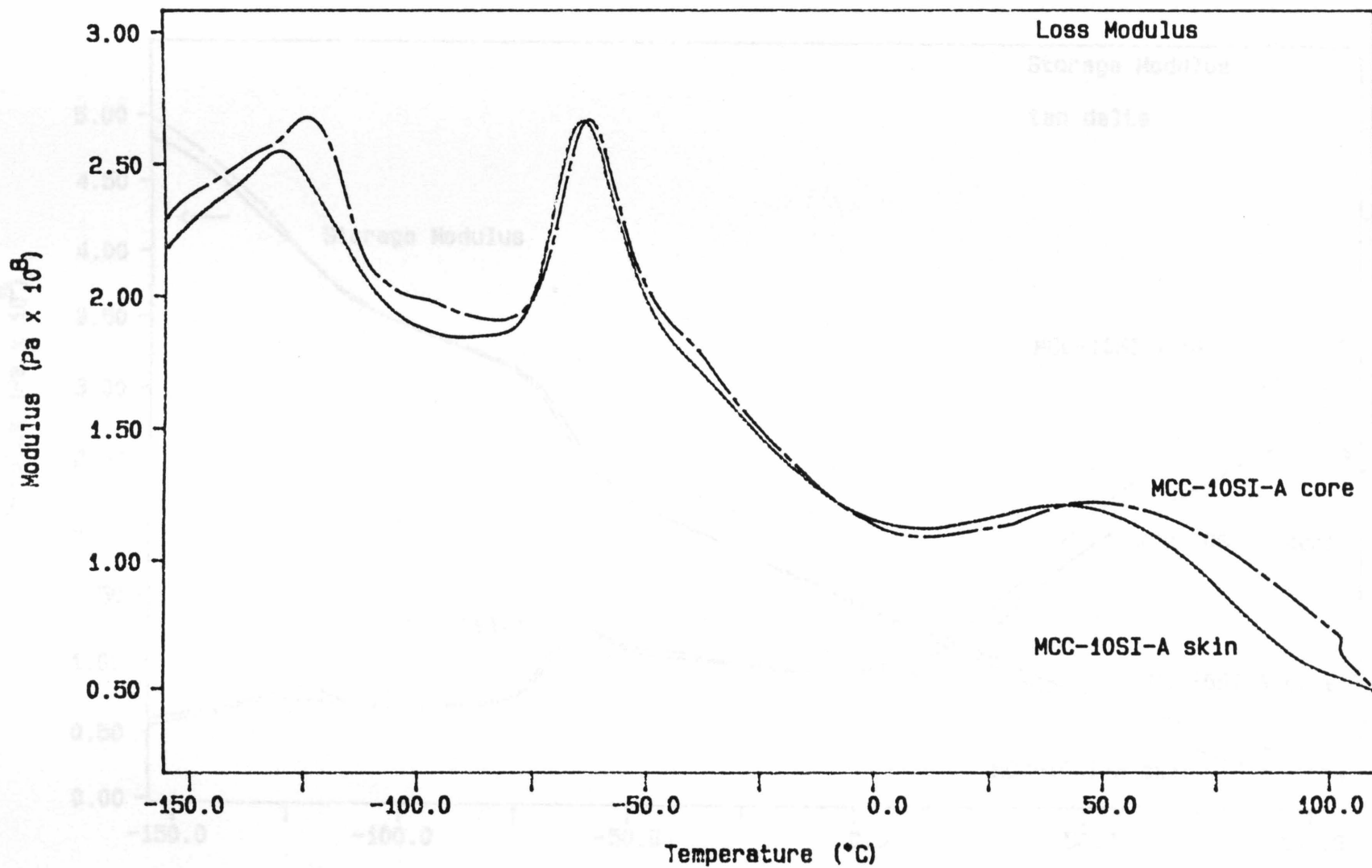
Figure 16a   DMA7 curves for MCC-10SI-A skin and core samples.
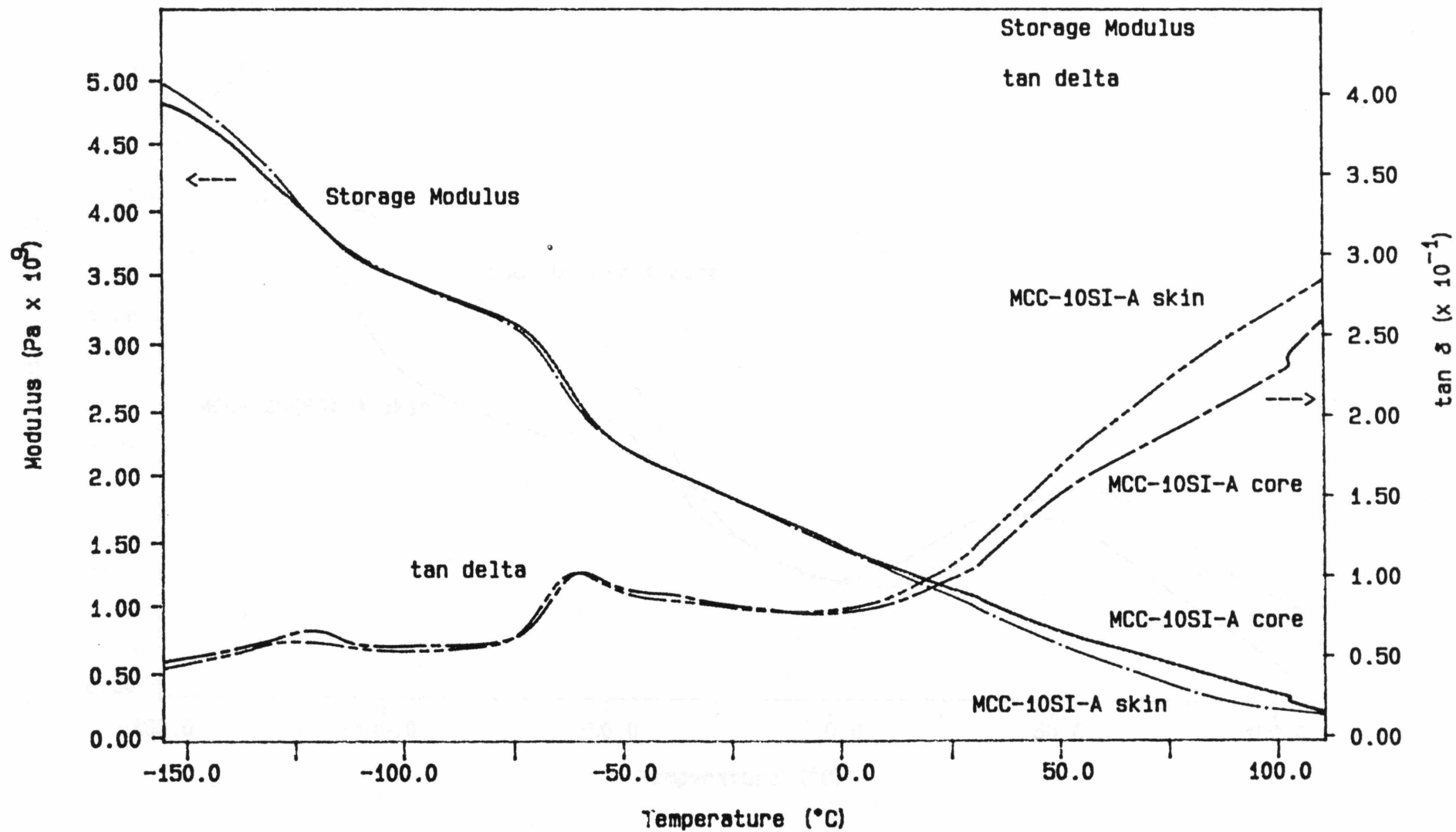
Figure 16b   DMA7 curves for MCC-10SI-A skin and core samples.
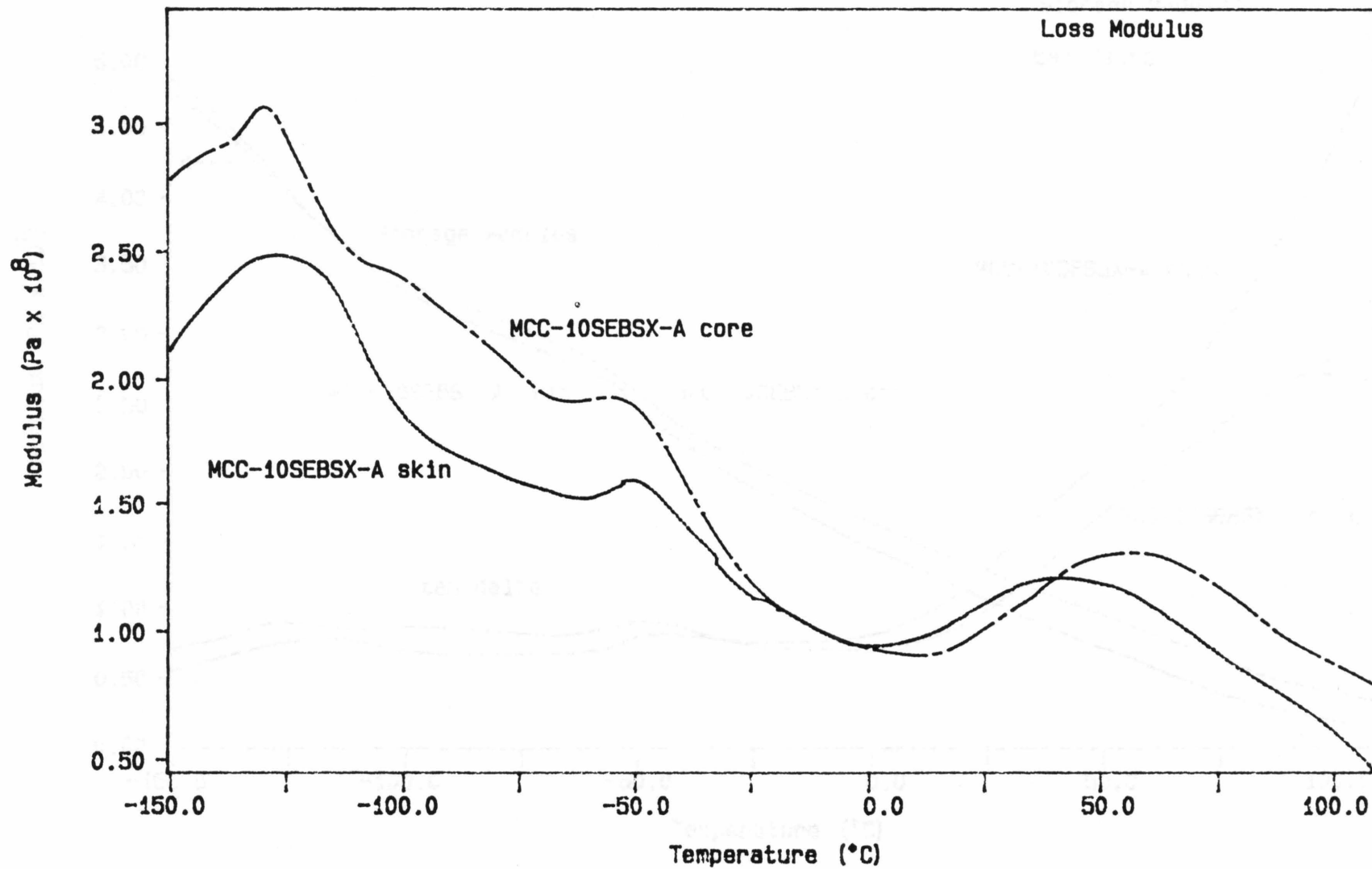
Figure 17a   DMA7 curves for MCC-10SEBSX-A skin and core samples.
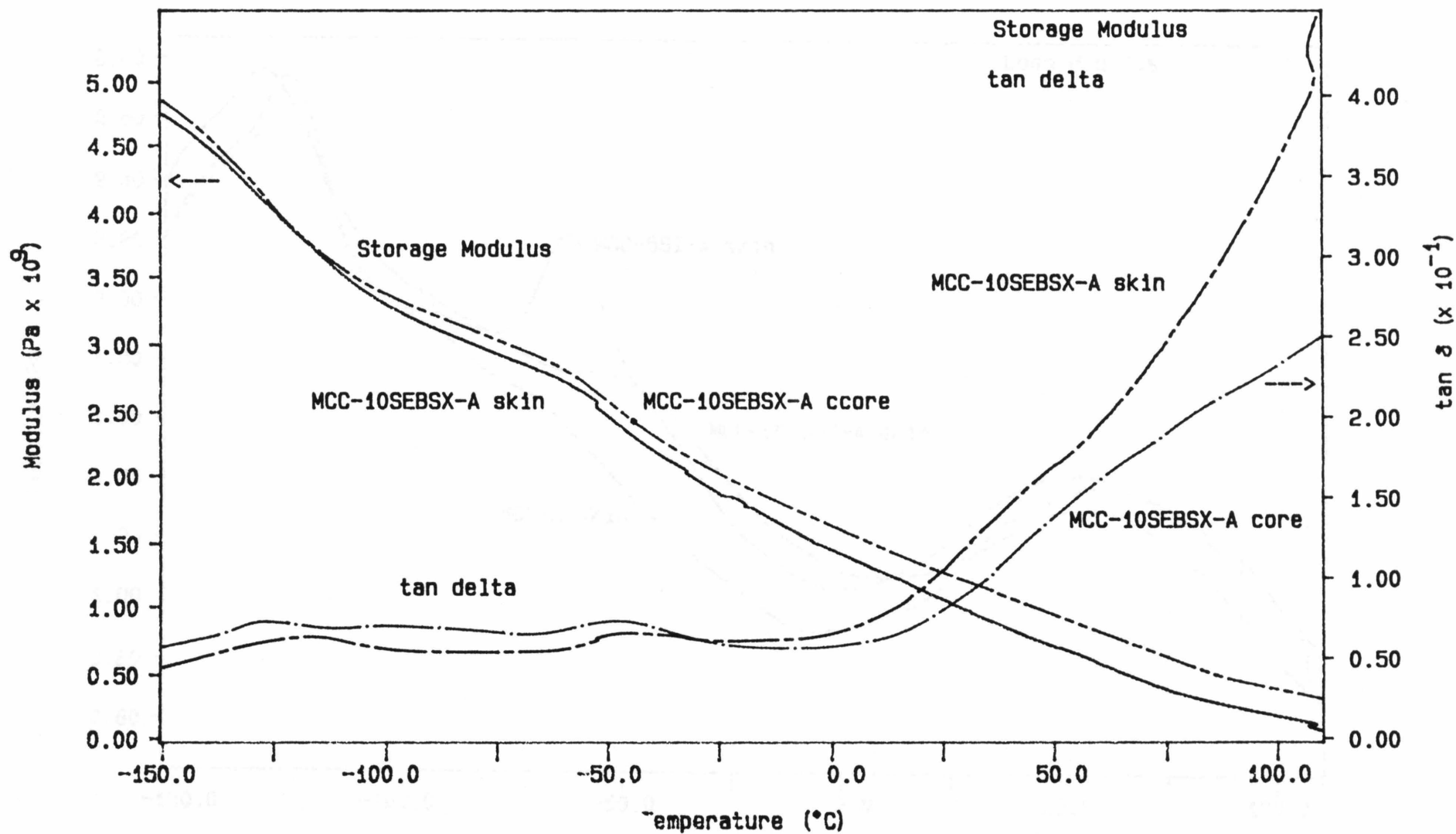
Figure 17b   DMA7 curves for MCC-10SEBSX-A skin and core samples.
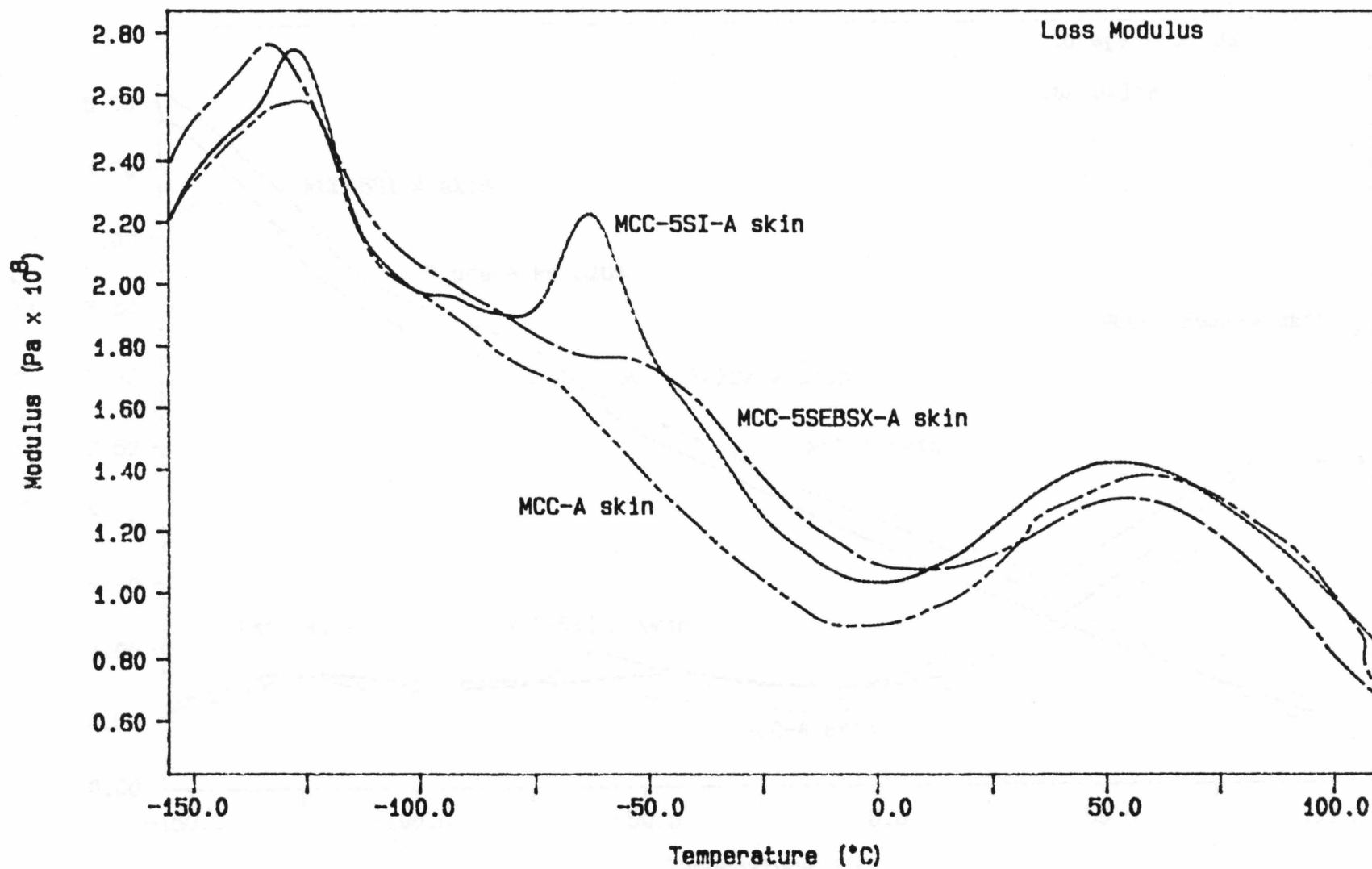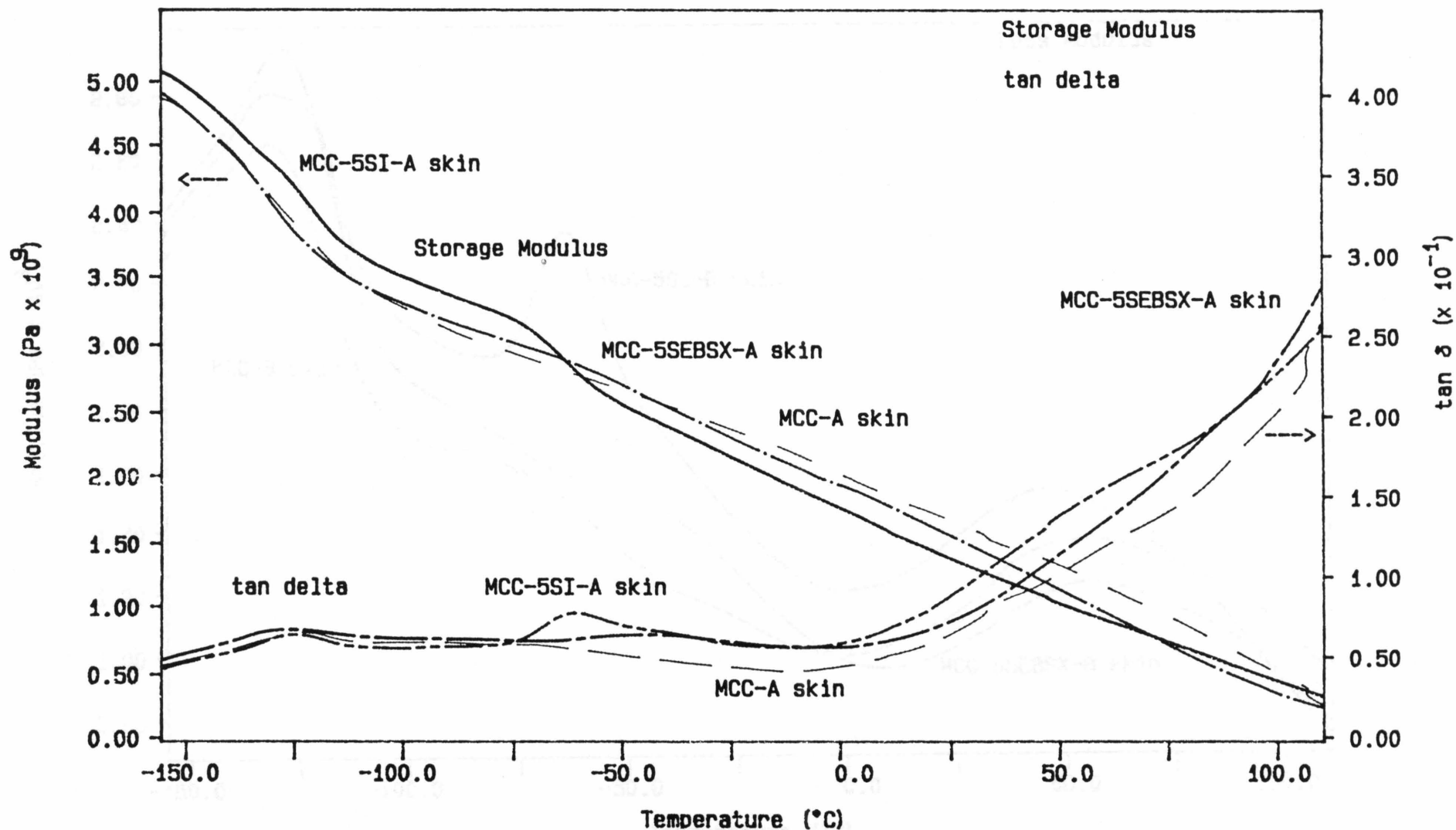
Figure 18a   DMA7 curves for the skin samples of MCC-A, MCC-5SEBSX-A, and MCC-10SI-A.   The glass transition of the isoprene block of the the SI elastomer, -70 to -50 °C) is very well defined for only 5% of the elastomer, suggesting enhanced interfacial adhesion at the PET/PE interface.   The transition is much less pronounced for MCC-5SEBSX-A.
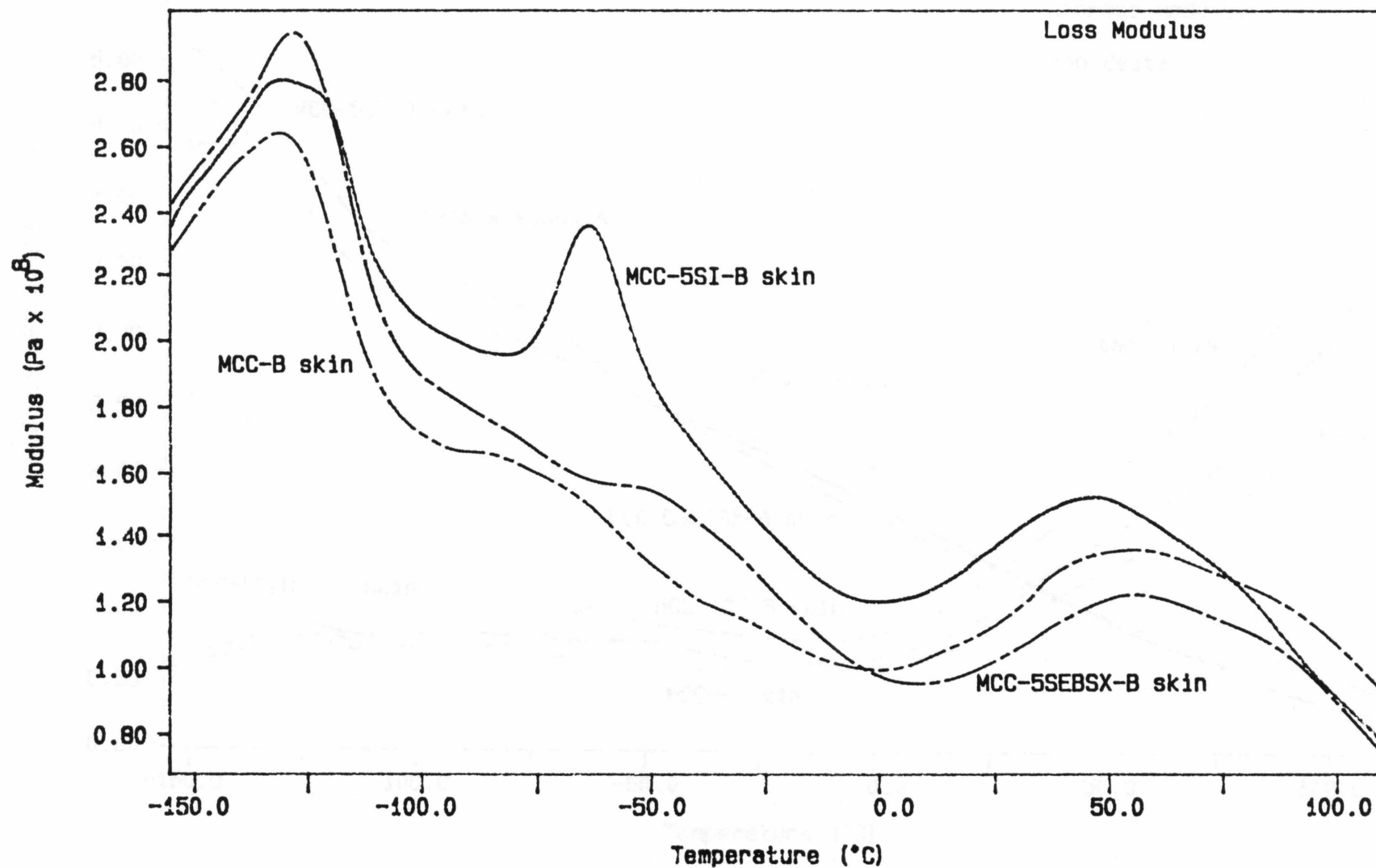
Figure 18b   DMA7 curves for the skin samples of MCC-A, MCC-5SEBSX-A, and MCC-10SI-A. The glass transition of the isoprene block of the the SI elastomer, -70 to -50 °C) is very well defined for only 5% of the elastomer, suggesting enhanced interfacial adhesion at the PET/PE interface. The transition is much less pronounced for MCC-5SEBSX-A.

Figure 19a   DMA7 curves for the skin samples of MCC-B, MCC-5SEBSX-B, and MCC-5SI-B.
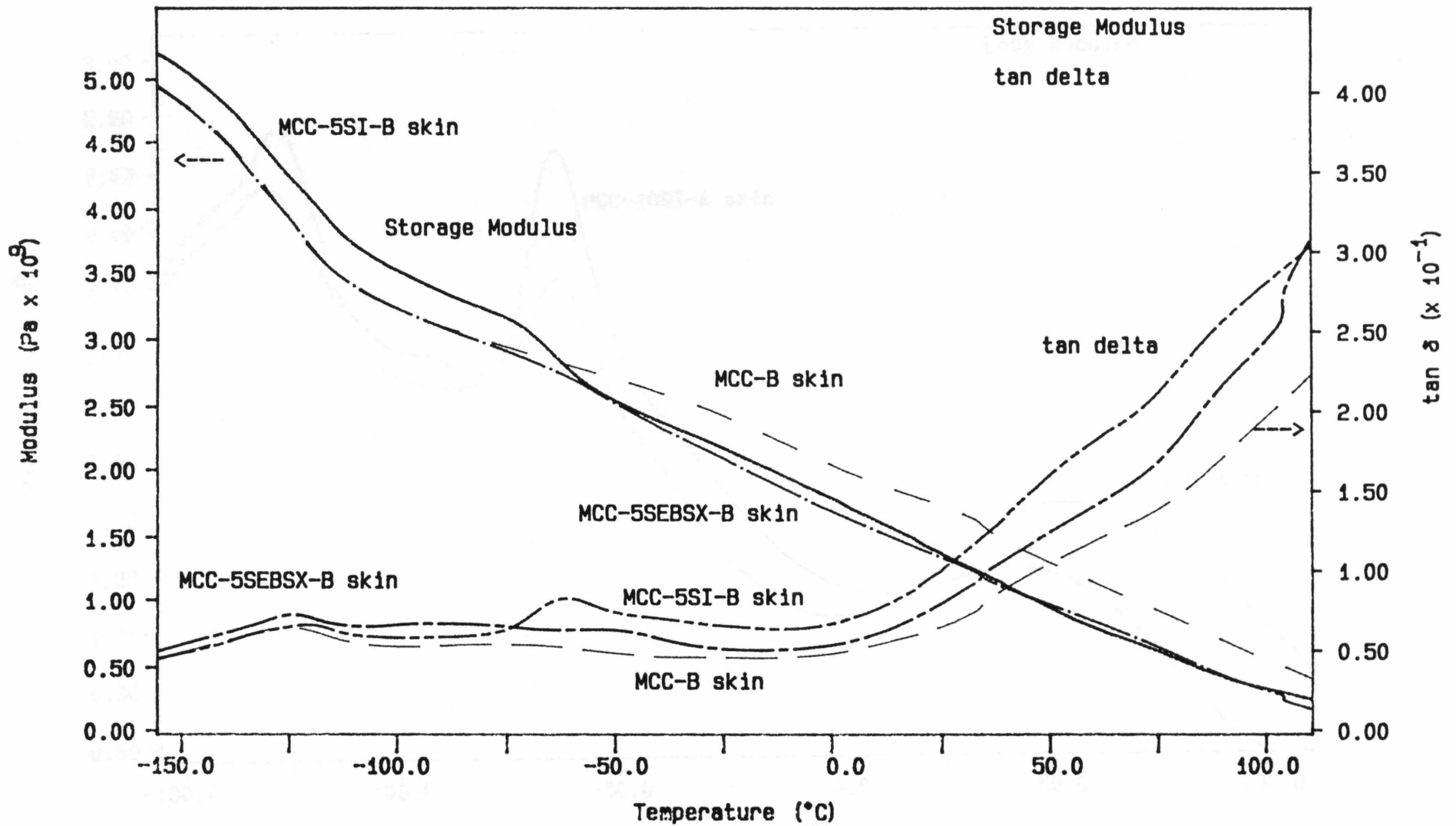
Figure 19b   DMA7 curves for the skin samples of MCC-B, MCC-5SEBSX-B, and MCC-5SI-B.
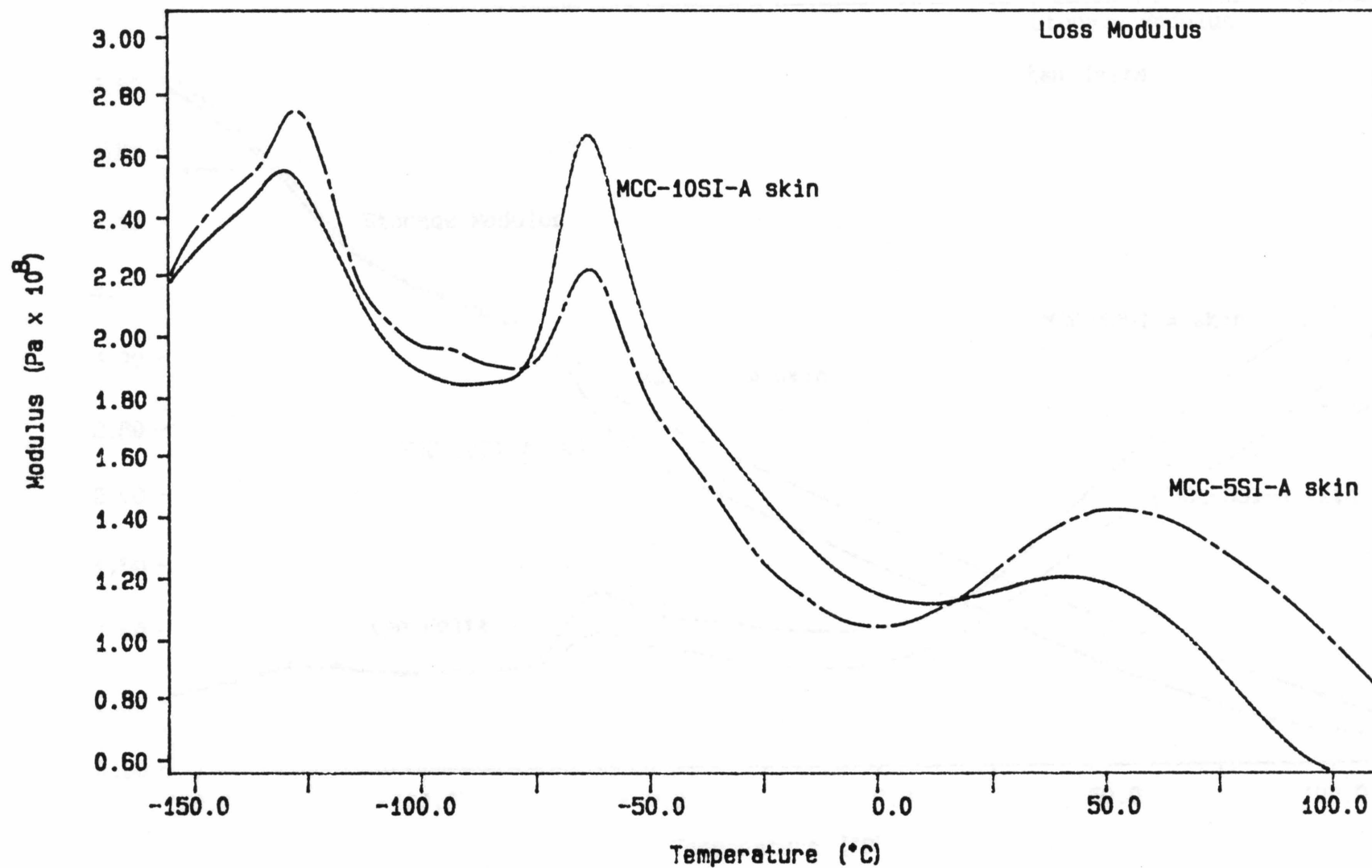
Figure 20a   DMA7 curves for the skin samples of MCC-5SI-A and
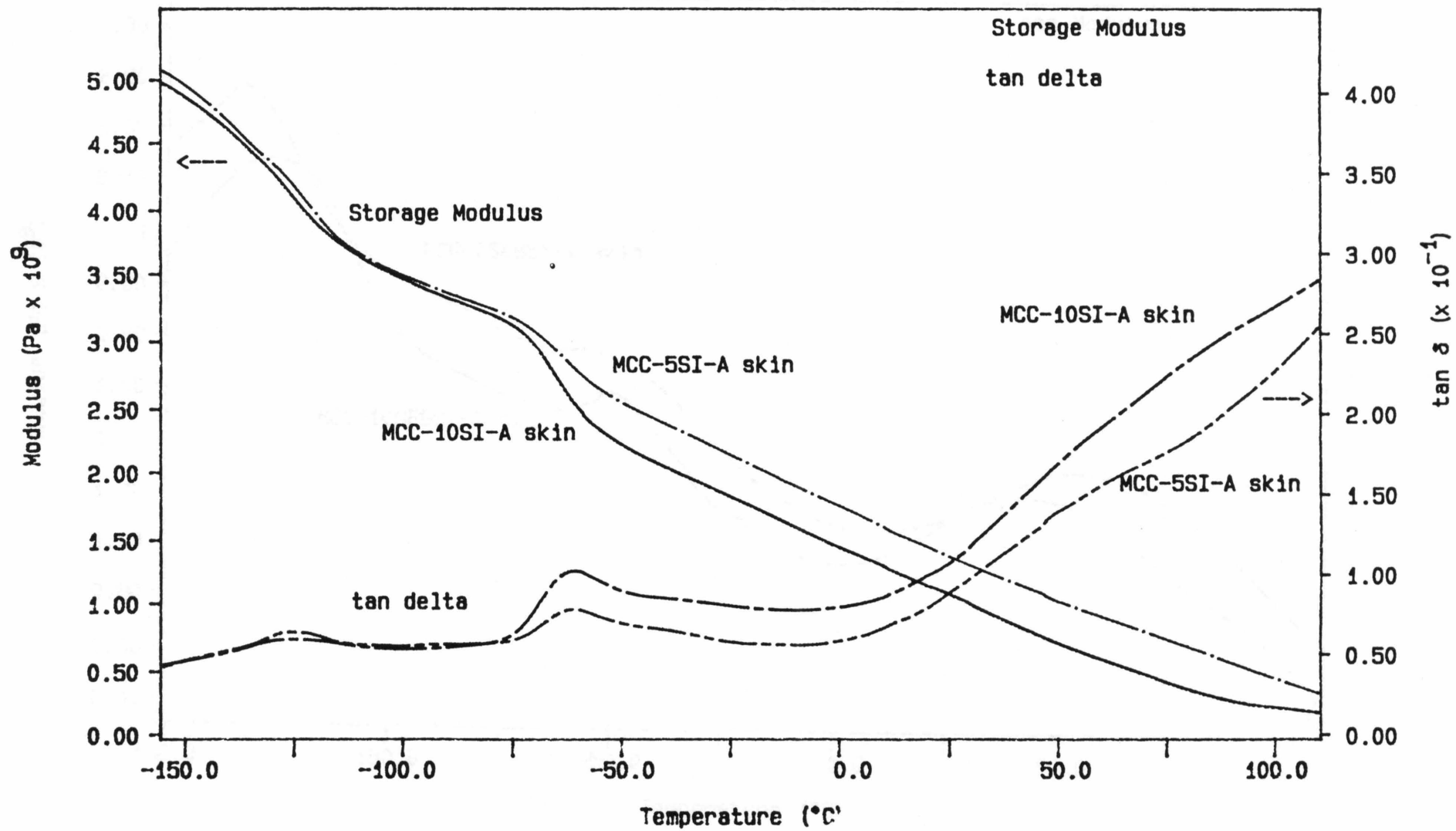MCC-10SI-A.

Figure 20b   DMA7 curves for the skin samples of MCC-5SI-A and MCC-10SI-A.
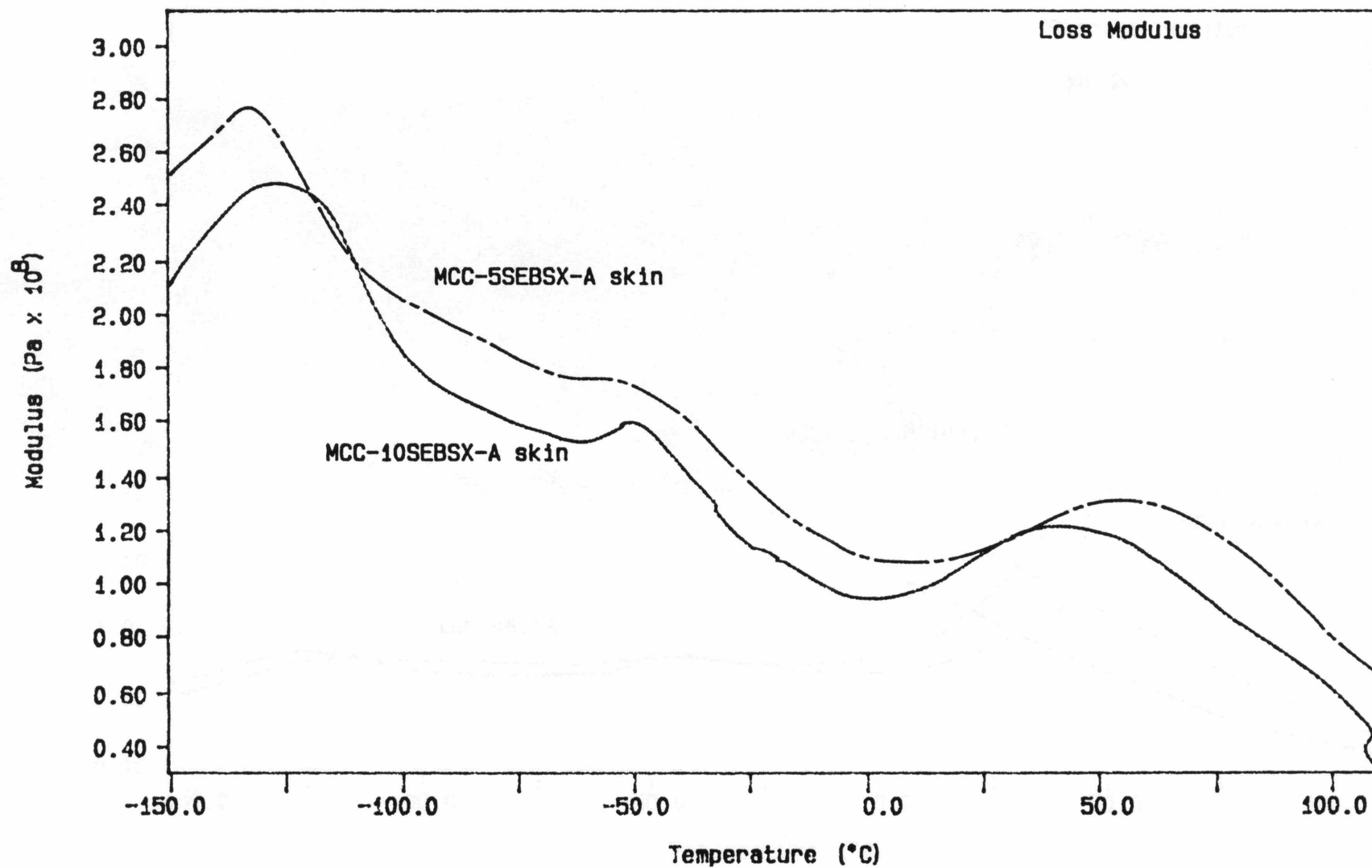
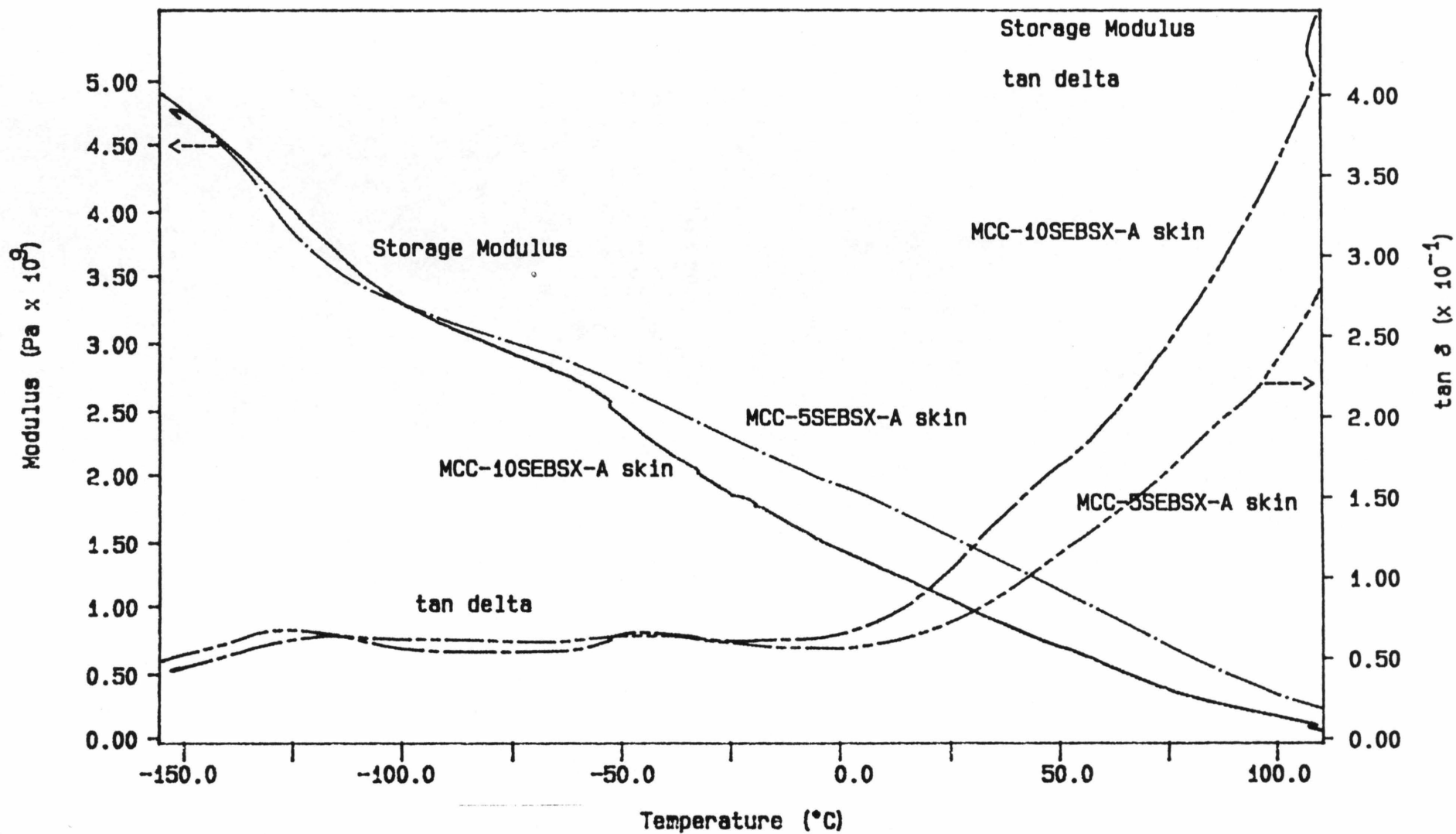Figure 21a   DMA7 curves for the skin samples of MCC-5SEBSX-A and MCC-10SEBSX-A.

Figure 21b   DMA7 curves for the skin samples of MCC-5SEBSX-A and
MCC-10SEBSX-A.